Stockholm University

Bachelor Thesis

Degree Project in
Earth Science, 15 hp

To be an eclogite or not? Insights from thermodynamic modelling

Elsa Lindström

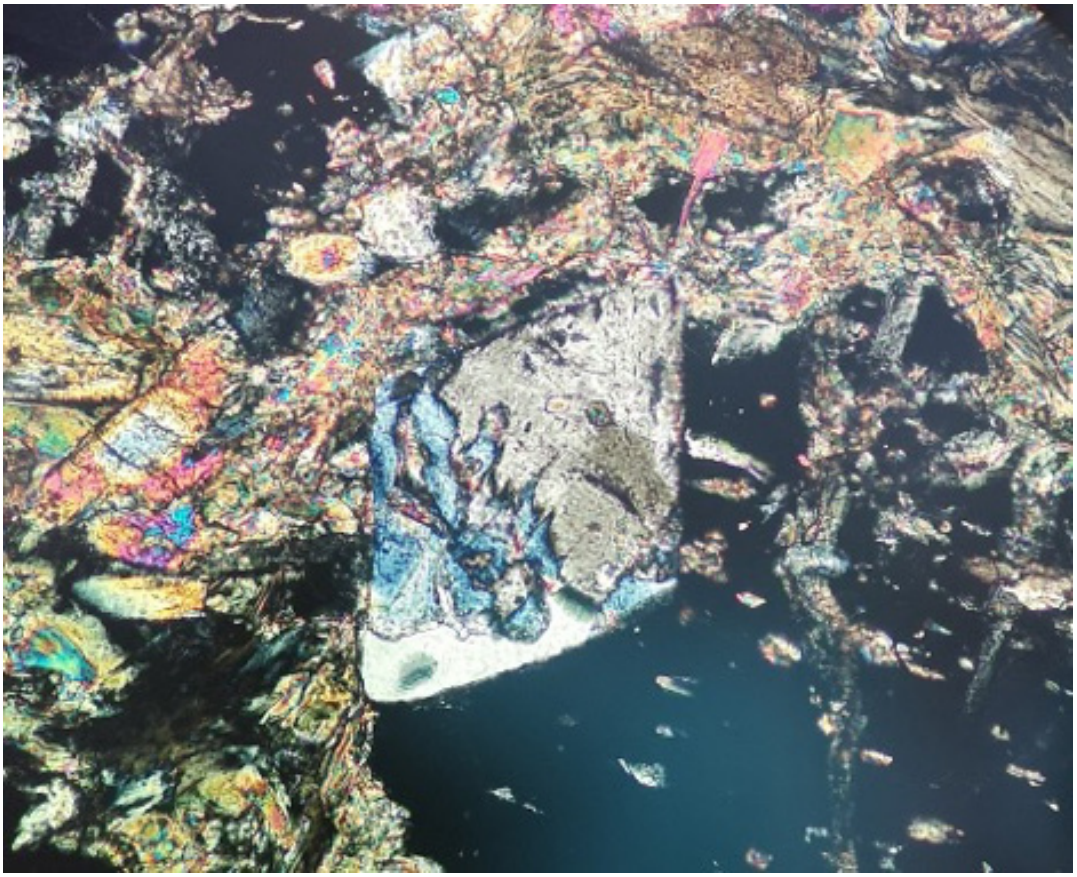

Stockholm 2026

Department of Geological Sciences
Stockholm University
SE-106 91 Stockholm

Abstract

The Western Alps hold some of the best exposed pieces of subducted oceanic lithosphere, specifically the units of the Piemonte-Liguria Ocean. These units record blueschist- to eclogite-facies metamorphism. Constraining the peak *P–T* conditions reached by the different fragments during the Alpine history provides key information to reconstruct the internal metamorphic and tectonic architecture of the Piemonte-Liguria Ocean, which remains debated. For instance, in the Western Alps, the contact between the blueschist Combin Zone and the eclogitic Zermatt Zone is disputed. This study uses petrography, mineral chemistry and thermodynamic modelling to re-evaluate the peak *P–T* conditions of a metabasalt, collected in in the Valtournanche valley (Western Alps). Some authors consider the sampling area as part of the eclogitic Zermatt Zone, whereas for other ones it belongs to the blueschist Combin Zone. Despite some discrepancies between the measured and the modelled garnet composition, thermodynamic modelling indicates peak *P–T* conditions of 14–17 kbar 460–500 °C for the investigated metabasalt. These conditions fall in the blueschist facies indicating that (i) the sampling area belongs to the Combin Zone and thus (ii) the contact with the Zermatt Zone is located structurally below the studied sample.

Table of Contents

1. Introduction

Application of equilibrium thermodynamics has been diligently used to understand and constrain metamorphic conditions (e.g., Manzotti et al., 2015, 2022). It allows the calculation of pseudosections (isochemical phase diagrams) and the prediction of stable mineral assemblages at different *P–T* (pressure and temperature) conditions. This application has become central for interpreting metamorphic rocks and reconstructing their *P–T* paths (Lanari and Duesterhoeft 2019).

The Western part of the European Alps offer an exceptional natural setting for applying these methods. Subducted fragments of the former Piemonte-Liguria Ocean are well preserved and record blueschist- to eclogite-facies conditions (Agard, 2021). Therefore, the Alps are considered one of the best places worldwide to study deep subduction processes.

Within the Piemonte-Liguria oceanic domain, two main metamorphic units are recognized. The Combin Zone which records blueschist-facies conditions (Dal Piaz et al. 2015; Manzotti et al. 2021), and the Zermatt Zone which have reached quartz- to coesite-eclogite facies metamorphic conditions (Reinecke et al. 1991; Groppo et al. 2009). The contact between these units is interpreted as a major metamorphic discontinuity (Ballèvre and Merle 1993), but its exact position is disputed. In addition, assessing the peak metamorphic conditions of the Combin Zone is difficult due to the strong retrogression at greenschist facies conditions and the rare occurrence of preserved high-pressure minerals (Negro et al., 2013 and references therein).

This BSc thesis investigates a sample (a metabasalt) collected in an area interpreted as part of either the eclogitic Zermatt Zone or the blueschist Combin Zone. By combining petrography, mineral chemistry and thermodynamic modelling, this study aims to constrain its peak *P–T* conditions and to shed light on the position of the tectonic contact between the Zermatt Zone and the Combin Zone, which represents one of the major metamorphic discontinuities in the Alps.

2. Geological setting

2.1 The Piemonte-Liguria Ocean in the Western Alps

The Western Alps (Fig. 1) comprise several units of oceanic and continental affinities (e.g. Dal Piaz et al. 2015; Manzotti and Ballèvre 2024). The oceanic units are considered to derive from the Piemonte Liguria Ocean, a slow-spreading small oceanic domain Jurassic in age, which was subducted during the late Cretaceous (Manzotti et al. 2014 and refs therein). Its closure was followed by the collision between the European and Adriatic plates which resulted in the formation of the Alpine chain.

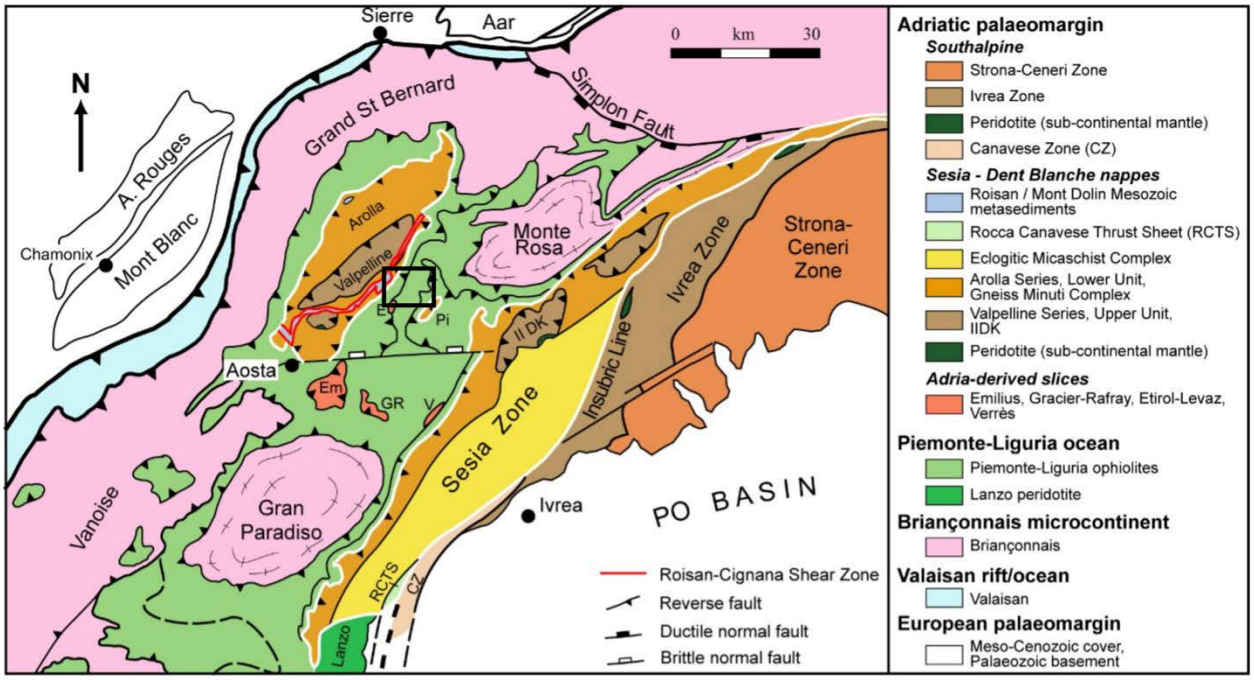

Fig. 1. Tectonic architecture of the Western Alps. The black rectangle indicates the sampling area in the Piemonte-Liguria Ocean (from Manzotti et al. 2014).

In the Alpine nappe stack, the oceanic units of the Piemonte-Liguria Ocean are located above the Internal Crystalline Massifs (Monte Rosa, Gran Paradiso and Dora-Maira Massif) and below the Sesia-Dent Blanche nappes (Fig. 2).

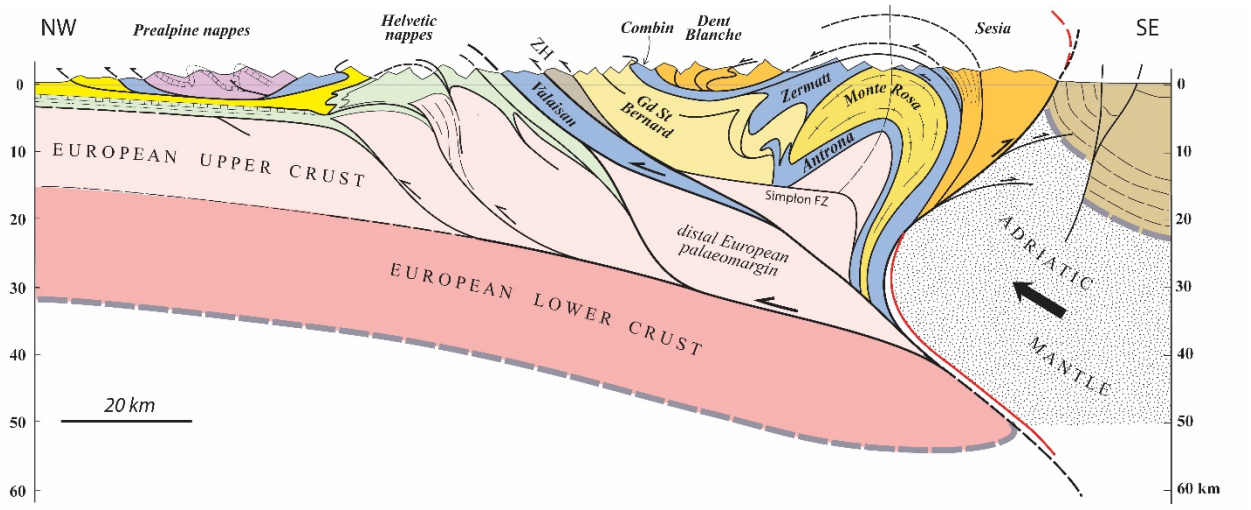

Fig. 2. Cross-section of the Western Alps showing the structural position of the oceanic Piemonte-Liguria Ocean units (blue color) with respect to the Alpine nappe stack (from Manzotti and Ballèvre 2024)

Overall, the oceanic units can be divided in two main groups on the basis of lithological, metamorphic and tectonic criteria (e.g. Dal Piaz et al., 2015; Agard 2021). The first group (type-I units) comprises units dominated by oceanic metasediments with minor ophiolites. By contrast, the second group (type-II) mainly consists of serpentinite, metagabbro, and metabasalt with minor metasediments. This lithological distinction is also associated with a difference in the peak metamorphic conditions reached during the Alpine subduction (e.g. Tajčmanová et al. 2021; Agard et al. 2021 and refs. therein). The type-I units equilibrated at low grade blueschist facies conditions (e.g. Bousquet et al., 2012; Manzotti et al. 2021), whereas the type-II units experienced eclogite facies conditions (e.g. Groppo et al., 2009; Dal Piaz et al. 2015).

2.2 Oceanic units in the Valtournanche valley

The *Valtournanche valley* in the Aosta Valley region exceptionally exposes oceanic units belonging to the Piemonte-Liguria Ocean. This N-S oriented valley is 25 km long, extending from Chatillon-Saint Vincent (this locality is not reported on the map of Fig. 3 because it is located more to the south) to Cervinia (Fig. 3).

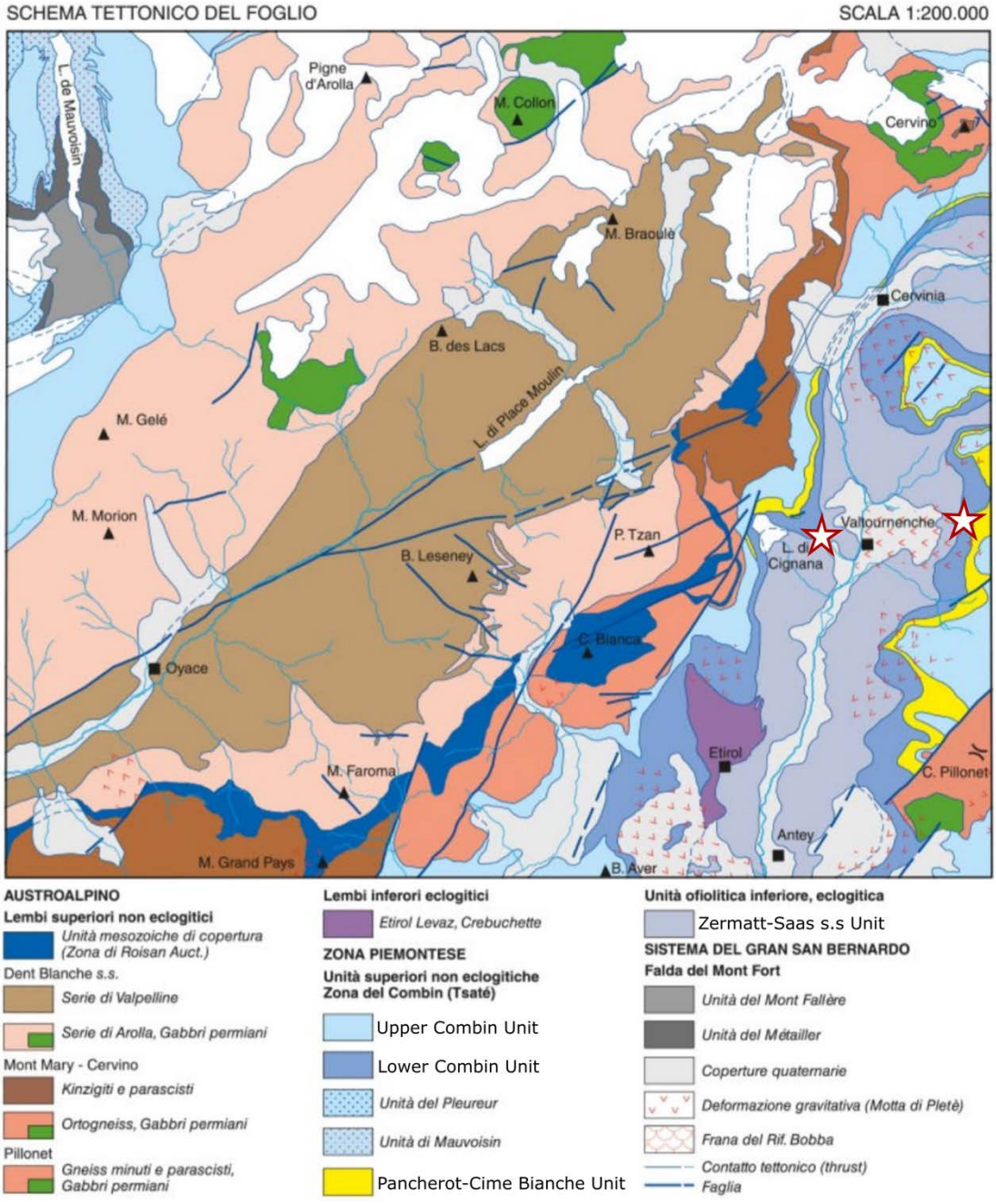

Fig. 3 Geological map of the left side of the Aosta valley, where the Valtournanche valley is located (modified from Dal Piaz et al. 2015). In the legend, the units belonging to the Piemonte-Liguria Ocean (here indicated as "Zona Piemontese") have been translated to English. The red stars refer to the position of the samples investigated in this BSc study.

From bottom to top, two main domains are recognized (Dal Piaz et al. 2015): the *Zermatt Zone* (made of type-II units) and the *Combin Zone* (made of type-I units).

The *Zermatt Zone* comprises serpentinite, metagabbro and metabasalt. In the Valtournanche valley, units belonging to this Zone equilibrated at quartz-eclogite or coesite-eclogite facies conditions (Reinecke et al. 1991, Groppo et al. 2009). Using thermodynamic modelling, Groppo et al. (2009) constrained the peak *P–T* conditions for two different units at 27–28 kbar 570–605 °C and >32 kbar 590–605 °C, in the quartz-eclogite and coesite-eclogite facies, respectively.

The *Combin Zone* comprises metasediments (mainly marlstone and limestone) associated with minor metabasalt, metagabbro and serpentinite. In the Valtournanche valley, several units have been recognized within the Combin Zone (Dal Piaz et al. 2015): the *Lower Combin Zone*, the *Pancherot-Cime Bianche Unit*, the *Upper Combin Zone* (Fig. 3). It is generally assumed that the Combin Zone reached peak blueschist facies conditions followed by a pervasive greenschist facies overprint (Dal Piaz et al. 2015; Manzotti et al. 2021), but very few petrological studies were performed. For instance, Negro et al. (2013) estimated the maximum *T* conditions at 420–530 °C by Raman spectroscopy on carbonaceous material. However, the maximum *T* could have been reached also during the retrograde greenschist facies overprint.

The contact between the Zermatt Zone and the Combin Zone is interpreted as a normal fault (the Combin Fault; Ballèvre and Merle 1993) or as an out-of-sequence thrust (Ring 1995). In the Valtournanche valley and specifically in the area of the Cignana Lake (Fig. 3), the position of this contact is disputed (Fig. 4). The difference in metamorphic conditions (i.e. eclogite facies for the Zermatt Zone and blueschist facies for the Combin Zone) have been used to trace the boundary between these two domains. Overall, two main interpretations have been proposed based on structural, metamorphic and lithological criteria (Fig. 4).

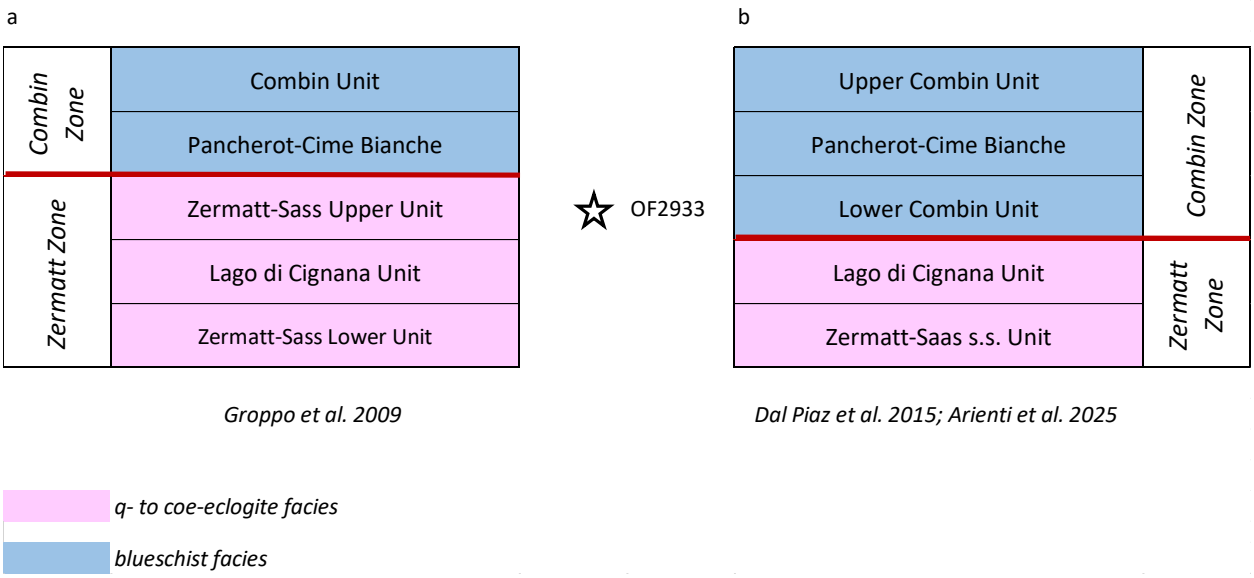

Fig. 4. Oceanic nappe stack in the Valtournanche valley according (a) to Groppo et al. (2009), and (b) to Dal Piaz et al. (2015) and Arienti et al. (2025). Note the difference position of the tectonic boundary (red line) between the Zermatt and Combin Zone. The white star refers to the structural position where the metabasalt (sample OF2933) studied by Groppo et al. (2009) was collected.

According to Groppo et al. (2009) the oceanic nappe stack in this area comprises from bottom to top: the Zermatt Sass Lower Unit, the Cignana Lake Unit, the Zermatt Saas Upper Unit, the Pancherot-Cime Bianche, and the Combin Unit. The main contact between the eclogite-facies Zermatt Zone and the blueschist-facies Combin Zone is therefore located just below the Pancherot-Cime Bianche (red line in Fig. 4a).

By contrast, according to Dal Piaz et al. (2015) and Arienti et al. (2025), the oceanic nappe stack comprises from bottom to top: the Zermatt-Sass s.s., the Lago di Cignana Unit, the Lower Combin Zone, the Pancherot-Cime Bianche and the Upper Combin Zone. The contact between the eclogite-facies Zermatt Zone and the blueschist-facies Combin Zone is therefore located just above the Lago di Cignana Unit (red line Fig. 4b).

Groppo et al. (2009) placed the contact between the Zermatt and Combine Zones below the Pancherot-Cime Bianche based on a thermobarometric study conducted on a metabasalt (sample OF2933) collected on the south slope of Mt. Pancherot close to the Cignana Lake (Fig. 3). This

sample contained chlorite, epidote, albite, garnet, phengite, minor quartz, amphibole, titanite, and carbonate. As clearly pointed by the authors, omphacite was not observed and no omphacite pseudomorphs were recognized. Garnet–phengite thermometer and the Si content in phengite (Krogh & Råheim 1978 and Green & Hellman 1982) were applied and returned peak metamorphic conditions of 24 kbar and 600 °C (Groppo et al. 2009). These *P–T* values plot within the field of the eclogite facies in a *P–T* space for metabasaltic system (see for comparison Fig. 5 and section "Metabasalts and the definition of metamorphic facies"), an argument used by Groppo et al. (2009) (i) to conclude that the studied sample belongs to the Zermatt Zone and thus (ii) to trace the contact with the Combin Zone above the collected sample (i.e. just below the Pancherot-Cime Bianche, Fig. 4a).

However, omphacite was not identified in the studied sample neither as preserved pristine mineral or as pseudomorph. Groppo et al. (2009) explained the absence of omphacite as a consequence of a high oxidation state during metamorphism. However, the whole Fe^{3+} content of the studied sample was not measured, rendering this hypothesis quite speculative. Alternatively, the authors proposed that the absence of omphacite can be the result of high value of CO_2 and low values of H_2O, as suggested by the presence of carbonate. In both cases, the stability field of blueschist facies assemblages is enlarged at the expense of eclogite facies assemblages.

The aim of this BSc thesis is to re-assess the peak *P–T* conditions of the rocks exposed at the same structural level than sample OF2933 (considered as part of the Zermatt Zone by Groppo et al. 2009 and as part of the Combin Zone by Dal Piaz et al. 2015 and Arienti et al. 2025, Fig. 4). Thermodynamic modelling (i.e. calculation of isochemical phase diagrams) will be applied on a metabasalt sample collected very close to OF2933, with the aim to provide new insights on the internal architecture of the Piemonte-Liguria Ocean and on the position of one of the major metamorphic discontinuity in the Western Alps.

3. Theory

3.1 Metabasalts and the definition of metamorphic facies

Pentti Eskola, a Finnish geologist, was the first to introduce the concept of metamorphic facies in 1915 and thus a way of classifying metamorphic rocks. He defined the facies by connecting (metamorphosed) mafic rocks composition and mineralogy to different conditions of *T* and *P*. The usage of basaltic rocks provided a means to compare metamorphic rocks around the globe, as basalts occur in most orogenic belts. Since the first introduction, research in the field of thermodynamics and experimental petrology has refined the concept and resulted in various subdivisions of metamorphic facies based on mineral assemblages. The distribution of these facies can be illustrated in *P–T* diagrams such as in Fig. 5, where each field represents the stability of a specific mineral assemblages. The lines are depicted as dashed lines because their exact position can slightly change as a function of the bulk-rock chemistry (including the fluids phase). This means that two different bulk-rock compositions can result in different mineral assemblages for the same *P–T* conditions. Thus, the facies boundaries provide a qualitative *P–T* estimates for a specific mineral assemblage (Winter, 2010; Manzotti and Ballèvre, 2024).

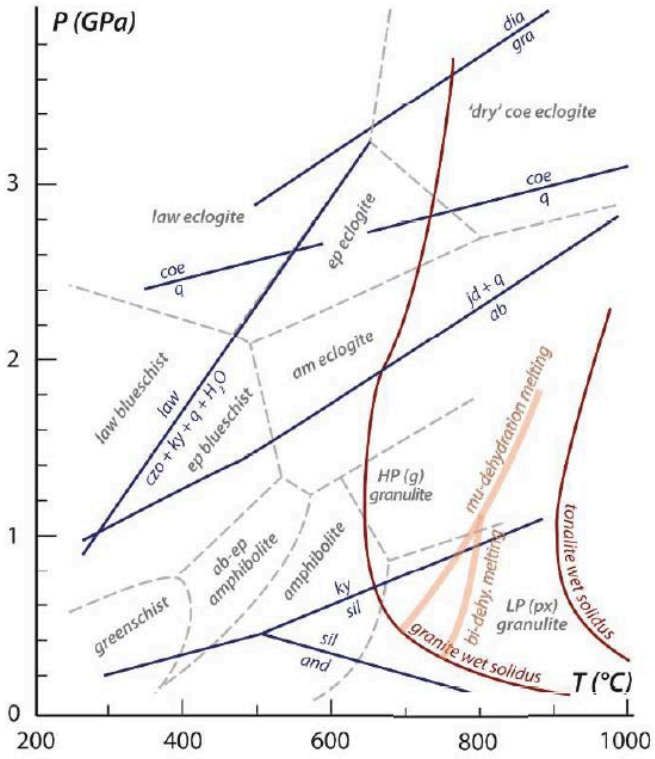

Fig. 5. *P–T* diagram showing the distribution of the major metamorphic facies, (from Manzotti and Ballévre, 2024)

Tab. 1 report the key-mineral assemblages for each metamorphic facies in a metabasite.

Metamorphic facies	Metabasites
greenschist	ab-chl-act-ep
law blueschist	gl-law-sph
ep blueschist	g-gl-ep-ru
law eclogite	law-cpx-g-ru
ep eclogite **am eclogite**	g-cpx-ru-q-am-ep
"dry" coe eclogite	g-cpx-ru-coe
ab-ep amphibolite	ab-chl-hb-ep
amphibolite	pl-hb-ilm
high-grade amphibolite	pl-hb-ilm
LP granulite	pl-cpx-opx-(hb)
HP granulite	pl-cpx-g-(hb)

Tab 1. Expected mineral assemblage for a metabasite at the different metamorphic facies (modified from Manzotti and Ballèvre, 2024).

Given that this study focuses on blueschist and eclogite facies, their main characteristics are briefly described below.

Metabasalts equilibrated at blueschist facies (Fig. 6a) are generally blue in color, due to the large abundance of glaucophane, a sodic amphibole (Philpotts & Ague 2022). The stable minerals in addition to glaucophane is given in Tab 1. At low *T* conditions, lawsonite and titanite also occur together with glaucophane (lawsonite blueschist). At higher *T*, epidote, rutile and glaucophane are observed (epidote blueschist). In Fig 5, the two facies are separated by the reaction law = czo + ky + q + H_2O (Manzotti and Ballèvre 2024). In the epidote blueschist facies, garnet is also present and forms from a reaction that mainly consumes lawsonite. Because the blueschist facies requires relatively low *T* and high *P* conditions, blueschists are associated with subduction zones, a tectonic setting which are characterized by low geothermal gradients (Bucher and grapes 2011). The eclogite facies field is quite large (Fig. 5) and it contains the minerals omphacite (a sodic-calcic clinopyroxene), garnet and rutile. This metamorphic facies can be subdivided into sub-facies based on the occurrence of key minerals, such as lawsonite, glaucophane, and epidote. These minerals are stable at different *P–T* conditions (Fig.5).

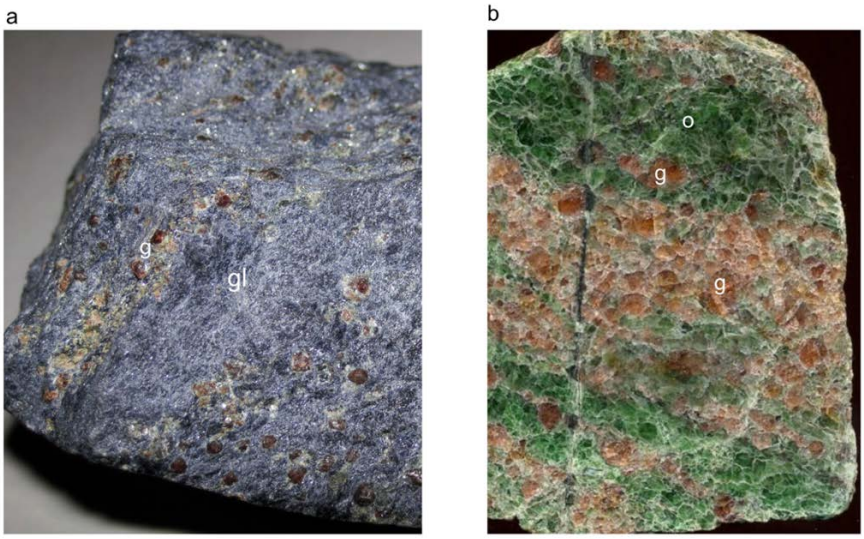

Fig. 6. a) Metabasalt equilibrated at blueschist facies containing the blue amphibole glaucophane (gl) and garnet crystals (g). Image from GeologyScience https://geologyscience.com/rocks/metamorphic-rocks/foliated-metamorphic-rocks/blueschist/. b) Metabasalt equilibrated at eclogite facies containing the green clinopyroxene omphacite (o) together with garnets (g). Image from Mindat https://www.mindat.org/photo-45288.html, copyright: Franz Bernhard).

The *P–T* conditions at which most eclogites equilibrated are constrained in the quartz stability field, at 16–18 kbar or 18–22 kbar depending on the geothermal gradient (Bucher and Grapes 2011). In addition, some eclogites equilibrated at ultra-high pressures (*UHP*) conditions, where minerals such as coesite (i.e. the SiO_2 polymorph) and even diamonds are stable, indicating *P* up to 40-50 kbar (Bucher and grapes 2011).

3.2 Macroscopic and microscopic identification, and P–T stability of some of the most common minerals in metabasalts

Garnet

Garnet, which is one of the most important metamorphic minerals, has the general structural formula $X_3Z_2(SiO_4)_3$. The X site can be filled by Ca, Mn, Fe^{2+} and Mg, giving rise to the major endmembers grossular, spessartine, almandine and pyrope, respectively (Spear 1993). These four endmembers form solid solutions with each other, therefore garnet often shows variations in chemical composition throughout a single grain. The concentration of each endmember is calculated from its proportional value in the structural formula. The Y site can incorporate Al, Fe^{3+} and Cr^{3+} (Spear 1993) although these substitutions are usually not included when recalculating the major garnet endmembers.

Garnets are often well preserved, displayed as euhedral crystals, a property which can be attribute to their hardness and resistance to weathering. The mineral appears in a variety of colors due to its diverse chemistry. For example, pyrope rich variants commonly appears pinkish red to purplish while almandine ones are red to brownish black. Optical properties of garnet include, in plane-polarized light, colorless to a slight pinkish hue and high relief (Fig. 7a). In crossed-polarized light, garnet is always extinct because it is isotropic (Fig 7b), (Deer, Howie, and Zussman 2013). Chemically, garnet crystals can be zoned. The zoning mainly reflects the change in *P* and *T* conditions during garnet growth (Konrad-Schmolke et al. 2005). If the chemistry throughout the grain is more uniform, no apparent zonation will be observed.

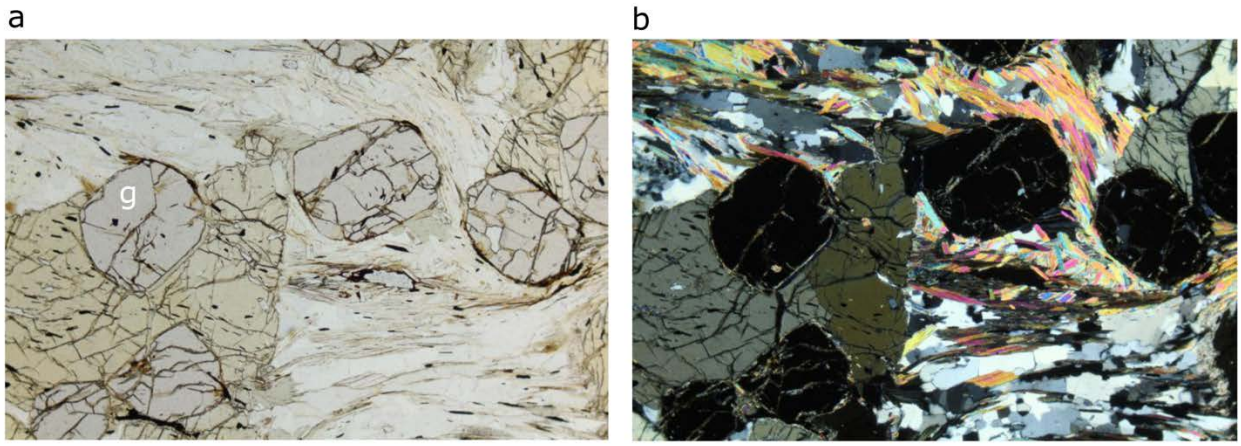

Fig. 7. a) The euhedral shape and high relief of garnet seen in microscope, plane polarized light. 2x (field of view 7 mm) b) Garnet is always extinct in crossed-polarized light due to its isotropic optical property. 2x (field of view 7 mm) Source for a) and b): from Alex Strekeisen https://www.alexstrekeisen.it/english/meta/garnet.php

Lawsonite

Lawsonite ($CaAl_2Si_2O_7(OH)_2 \cdot H_2O$.) is a metamorphic mineral that contains a large amount of water, up to 12 wt.%. The mineral has a characteristic lozenge or prismatic shape (Fig. 8a) and can appear as white to slightly pinkish in hand sample. Under the microscope, lawsonite appears as colorless in plane polarized light and exhibits first-order birefringence in crossed-polarized light together with a moderate relief. The mineral also commonly exhibits twinning and has two cleavages. The preservation of lawsonite is strongly dependent on the *P* and *T* evolution followed by a rock during exhumation. Lawsonite, therefore, has the best chance of being preserved if the *T* during retrogression remains low (Çetinkaplan et al. 2008) otherwise, it will break down and appear as lozenge shaped pseudomorphs (Manzotti et al. 2021). These pseudomorphs can contain white micas, (muscovite and/or paragonite), chlorite, and epidote (Ballèvre et al. 2003; Manzotti et al. 2021). Reactions (1) and (2) represent some examples of lawsonite breakdown.

(1) Lawsonite + glaucophane + garnet = chlorite + epidote + paragonite + vapor (Ballevre et al. 2003) .

(2) Lawsonite + garnet + K-bearing fluid = clinozoisite + chlorite + phengite (Schulte and Sindern 2002).

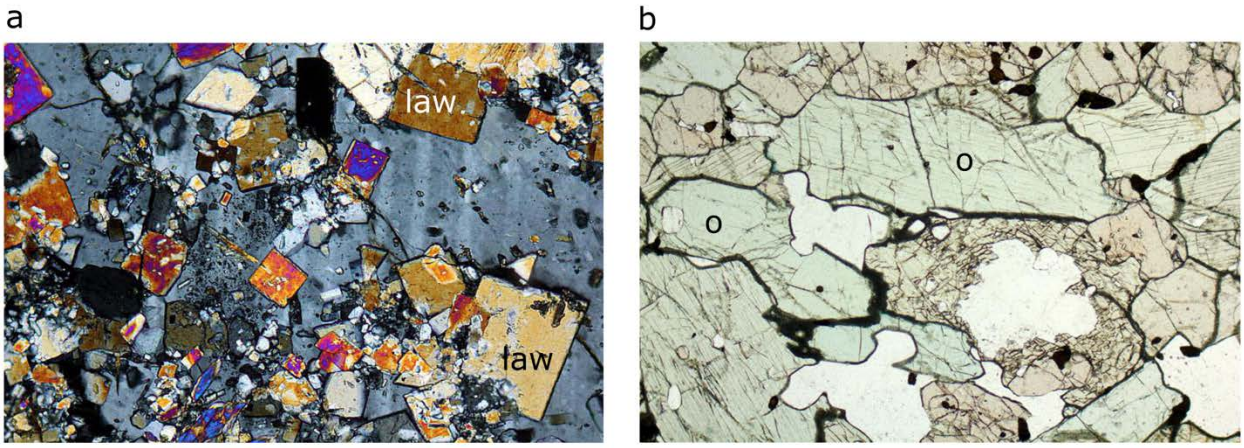

Fig. 8. a) Lawsonite crystal displaying a lozenge shape. Cross-polarized light, 10x (field of view 2 mm) source: Alex Strekeisen https://www.alexstrekeisen.it/english/meta/lawsonite.php b) Pale green color of omphacite in plane polarized light. Plane polarized light, 2x (field of view 7 mm) source: Alex Strekeisen https://www.alexstrekeisen.it/english/meta/omphacite.php

Omphacite

Omphacite, (Ca,Na) (Mg,Fe^{2+}, Fe^{3+},Al)Si_2O_6, belongs to the sodic-calcium subgroup of clinopyroxenes and can be considered as a solid solution between jadeite ($NaAlSi_2O_6$) and Fe-rich diopside ($CaMgSi_2O_6$) together with components of aegirine and calcium-aluminum clinopyroxenes. Omphacite shows a distinct green color in hand sample (Fig. 6b), which often translates to a pale green color in thin sections (Fig. 8b). The mineral has the characteristic pyroxene cleavage with grains of moderate relief. The birefringence colors are of the 2^{nd} order, and the mineral often appears in association with garnet, as omphacite is the diagnostic phase of eclogite facies rocks. During retrogression, a more calcic composition of omphacite can form as it breaks down, and the presence of fluids can result in the mineral transitioning into amphibole or symplectites of diopside and plagioclase (Dey et al. 2023).

4. Methods

4.1 Optical microscopy

Two metabasalt samples (VT2409B and VT2415B) were studied under the microscope and the mineral assemblages were determined through their optical properties. As mentioned above, these samples were collected at the same structural level as the OF2933 metabasalt sample from Groppo et al. (2009).

The percentage of garnet was calculated with ImageJ software and microphotographs of relevant minerals and microstructures were taken with LEICA Application Suit (LAS) EZ.

4.2 Electron microprobe (EPMA)

Electron Probe Microanalysis (EPMA) was performed on the key minerals, garnet, amphibole, white mica, chlorite and Fe-oxide in sample VT2409B at Uppsala Geocentrum (Fig. 9.) using both wavelength-dispersive spectrometers (WDS) and Energy-dispersive spectrometers (EDS).

Fig. 9. Electron microprobe at Uppsala Geocentrum the 27 april 2026.

EPMA utilize wavelength-dispersive spectrometers (WDS) and Energy-dispersive spectrometers (EDS) to provide insight of minerals chemical composition. The sample is bombarded by an electron gun, as it sits in a vacuum chamber, resulting in the elements emitting radiation which the spectrometers analyze. All elements have its unique electron configuration in orbitals and with the bombardment, the minerals electrons transition and energy are released. This energy works as a signature for each element and the chemical composition or identification of the mineral can be decided.

WDS and EDS operate at different spectral resolutions and precision, with WDS having a higher theoretical resolution limit at around 10eV, compared to EDS which limit lies at around 120eV. WDS therefore provide quantitative data of elements, including minor and trace elements, distribution, and concentration in minerals. Whilst EDS provide quick analysis of major elements and possible mineral identification. Both spectrometer techniques are useful and complement each other.

Samples analyzed with EPMA should prior to the analysis be coated with a 10–15 nm thick conductive layer of carbon, e.g., graphite. Uncoated samples cannot be electronically charged which results in a failed analysis, likewise an overcoated sample will give skewed data. Several analyses can be made on the same minerals in a sample without compromised quality as the EPMA is a non-destructive method (Cameca EPMA Tutorial).

The investigated thin section (sample VT2409B) was coated with a graphite layer estimated to be 17 nm thick by comparing a together coated brass coin to a set of standards. 17 nm is thicker than the generally accepted limit, which was described above as being 15 nm, however it was still regarded as a satisfactory coating for running analysis by the EPMA operator.

4.3 Bulk rock chemistry

The major bulk-rock composition for sample VT2409B was measured by inductively coupled plasma atomic emission spectrometry (ICP-AES; SARM-CRPG, Nancy). Details about the method are reported in Manzotti et al. 2020 Carignan et al. 2001. This method is used to measure the major elements of the rock but does not allow distinguishing between ferrous (Fe^{2+}) and ferric (Fe^{3+}) iron. Therefore, separate analyses for Fe^{2+} was conducted by a titration method using potassium dichromate ($K_2Cr_2O_7$). This method involves dissolving the sample in a hydrofluoric acid and sulfuric acid mixture (HF-H_2SO_4) together with boric acid (H_3BO_3) and phosphoric acid (H_3PO_4) before the titration. By acquiring the Fe^{2+} content from the rock the amount of Fe^{3+} can be calculated.

4.4 Thermodynamic modelling

Thermodynamic modelling was performed in order to calculate a pseudosection, which is an isochemical phase diagram (i.e. a diagram that is valid and built for a specific bulk rock composition). A pseudosection displays the stable mineral assemblages in a *P–T* space of interest. Theriak/Domino (de Capitani & Brown, 1987; de Capitani & Petrakakis, 2010) was used for the modeling's calculation together with the dataset ds6.2 and solid solution mixing models from Holland & Powell 2011. Calculations were performed in the chemical system $Na_2O - CaO - FeO - MgO - Al_2O_3 - SiO_2 - H_2O - TiO_2 - Fe_2O_3 \pm MnO \pm K_2O$ (MnNCKFMASHTO) in the *P–T* range 400–600 °C and 12–25 kbar. For the calculation H_2O was also considered to be in excess.

5. Results

5.1 Petrography

Sample VT2409B

The sample contains amphibole, epidote, quartz, garnet (~7%), chlorite, white-mica and biotite. There are also accessory minerals throughout the sample, including titanite, Fe-oxide, rutile, and zircon. The main matrix foliation is defined by the alternation of two different domains: type I domain (Fig 10a), which has a larger amount of chemically zoned epidote grains, and type II (Fig 10b), which consists of chlorite, blueish-green amphibole.

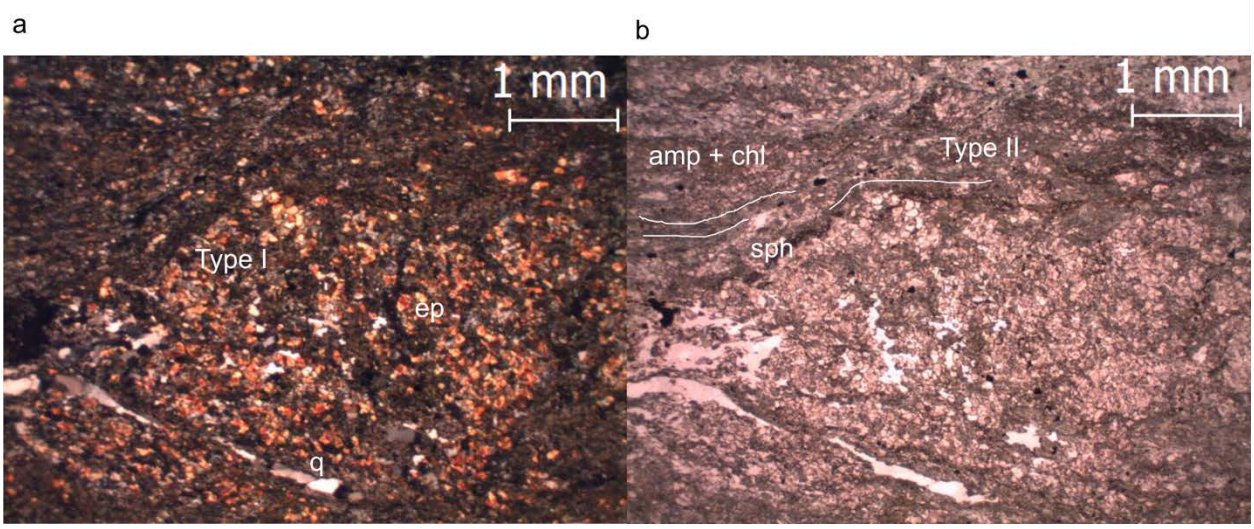

Fig. 10. Microscopic aspects of sample VT2409B. (a) An aggregate of epidote found in the type I domain. (b) Type II with the amphibole and chlorite assemblage. The white lines indicate the foliation. Bands of titanite can also be observed.

The main foliation is also defined by discontinuous bands of broken titanite grains. Overview of the rocks structure can be seen in the scan of the thinsection (Fig. 11)

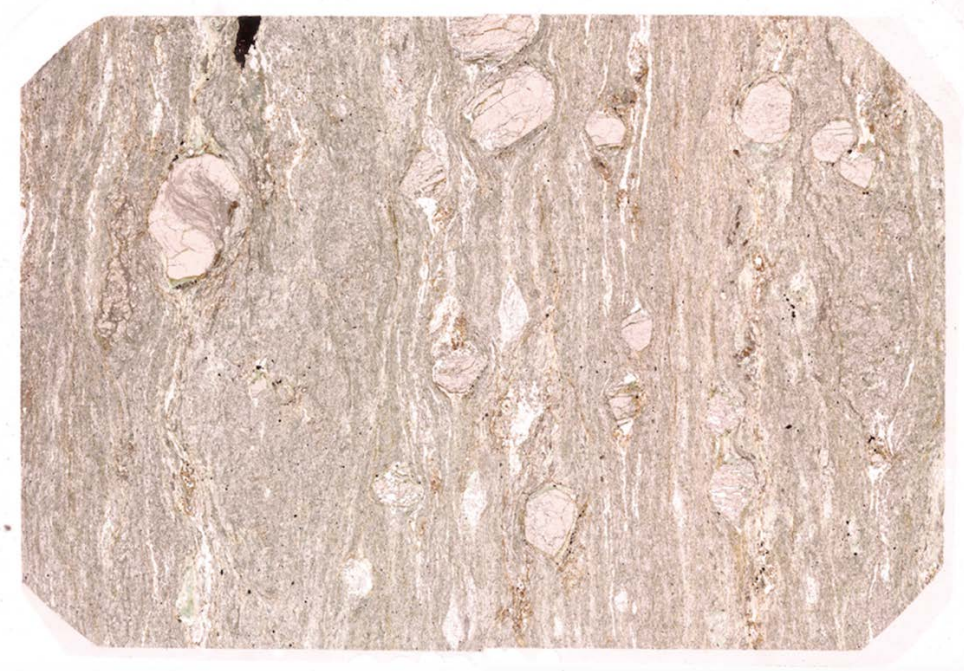

Fig. 11 Scan of the thin section VT2409B in plane polarized light (size of the thin section 4.5 x 3.0 cm).

The main foliation wraps around garnet porphyroblasts (up to 3 mm in size) and aggregates of white mica, with a characteristic lozenge shape (Fig. 12). These are interpreted as lawsonite pseudomorphs. Some of these more rigid structures have strain shadows of quartz and chlorite. The quartz is otherwise mainly found as bands stretching out from these strain shadows.

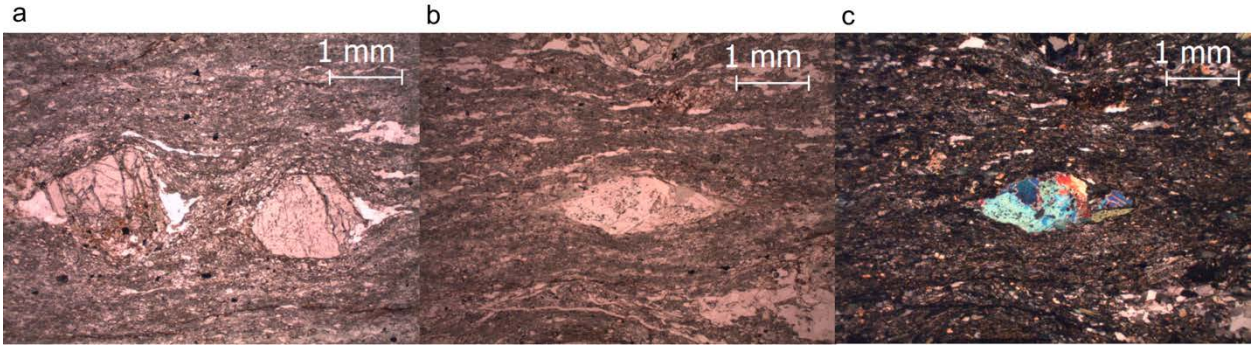

Fig. 12. a) Foliation wrapping around two garnet crystals which also display strain shadows of quartz. b) and c) Lozenge shape of white mica aggregates wrapped by the main matrix foliation (plane polarized light and crossed-polarized light respectively).

The garnet porphyroblasts of this sample are partially replaced at the rim by chlorite, and minor biotite. The garnets have inclusions of epidote, quartz, titanite, and locally rutile (Fig. 13a). In addition, microinclusions of zircon also occur. These inclusions define an internal foliation with trails that are either straight or slightly curved (Fig. 13).

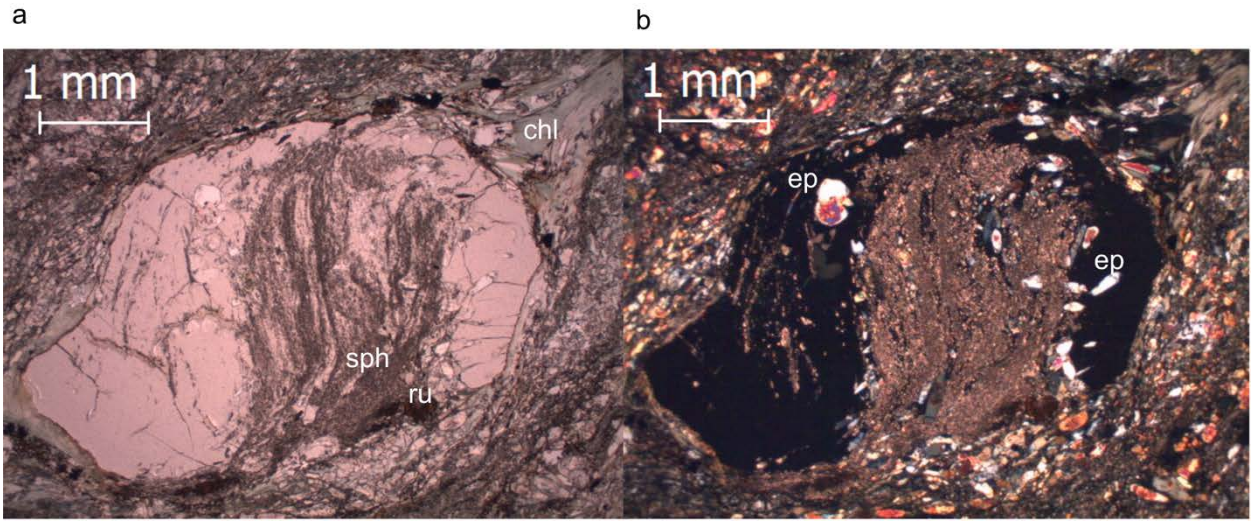

Fig.13. Garnet porphyroblast with inclusions of epidote, titanite and rutile in a) plane polarized light and b) crossed-polarized light. The inclusions defined a curved trail.

Sample VT2415B

Similar to VT2409B, sample VT2415B also contains amphibole, epidote, quartz, calcite, chlorite, garnet (~5%), white mica, biotite and accessory titanite and Fe-oxide. The rock has a banded structure, and the main foliation is defined by the alternation of two different domains (Fig. 14).

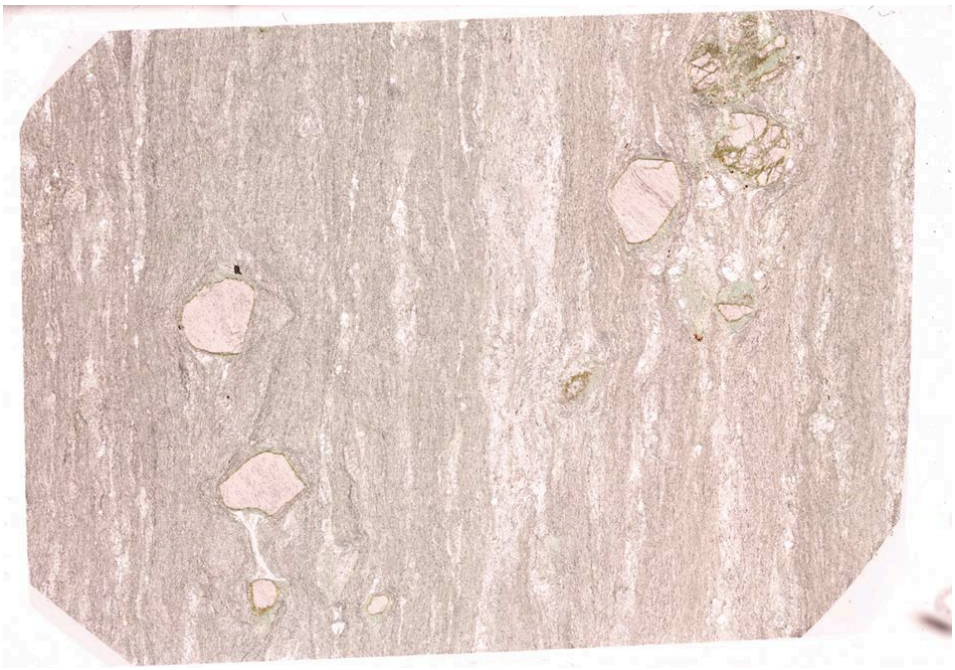

Fig 14. Scan of VT2415B in plane polarized light (size of the thin section 4.5 x 3.0 cm).

Type I domain is coarse-grained and mainly contains epidote, white mica, and calcite (Fig. 15a). Type II domain is fine-grained and mainly consists of chlorite, bluish-green amphibole, and white mica (Fig. 15b). Titanite-rich bands are also oriented parallel to the foliation.

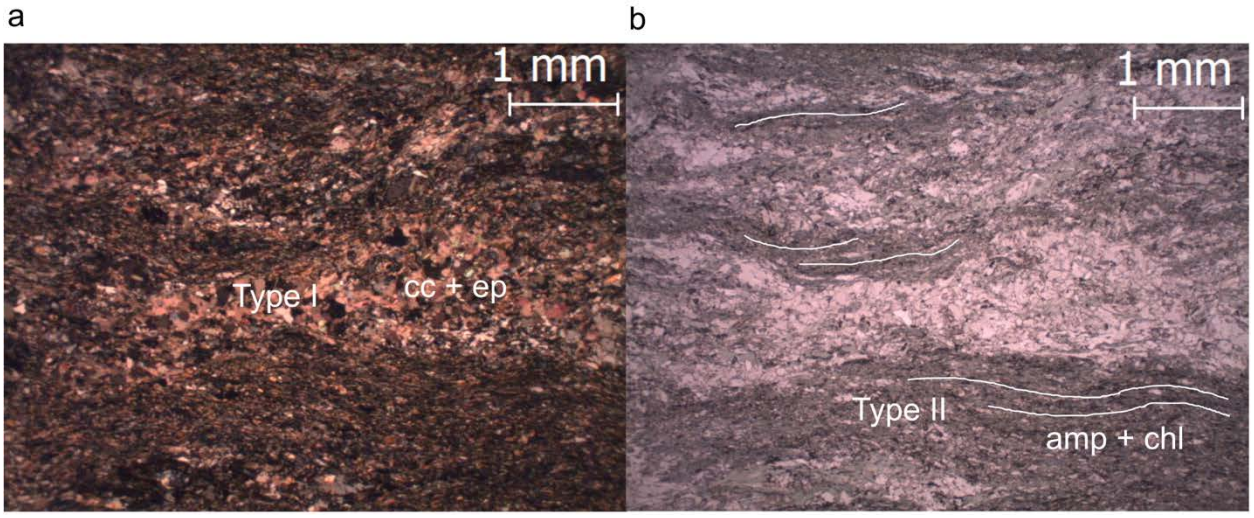

Fig.15. Microscopic aspects of sample VT2415B. (a) Type I domain consisting of epidote, calcite, and quartz. Microphotograph taken in cross-polarized light. (b) The main foliation (white lines) is marked by amphibole and chlorite concentrated in type II domain. Microphotograph taken in plane polarized light.

The main foliation wraps around garnet porphyroblasts (1.5–2 mm in size). The latter contain perfect lozenges which contain epidote, albite and tiny crystals of titanite (Fig. 16). These lozenges are interpreted as pseudomorphs after lawsonite. Garnet also contains inclusions of epidote and titanite. The garnet porphyroblasts of VT2415B are also more altered by chlorite.

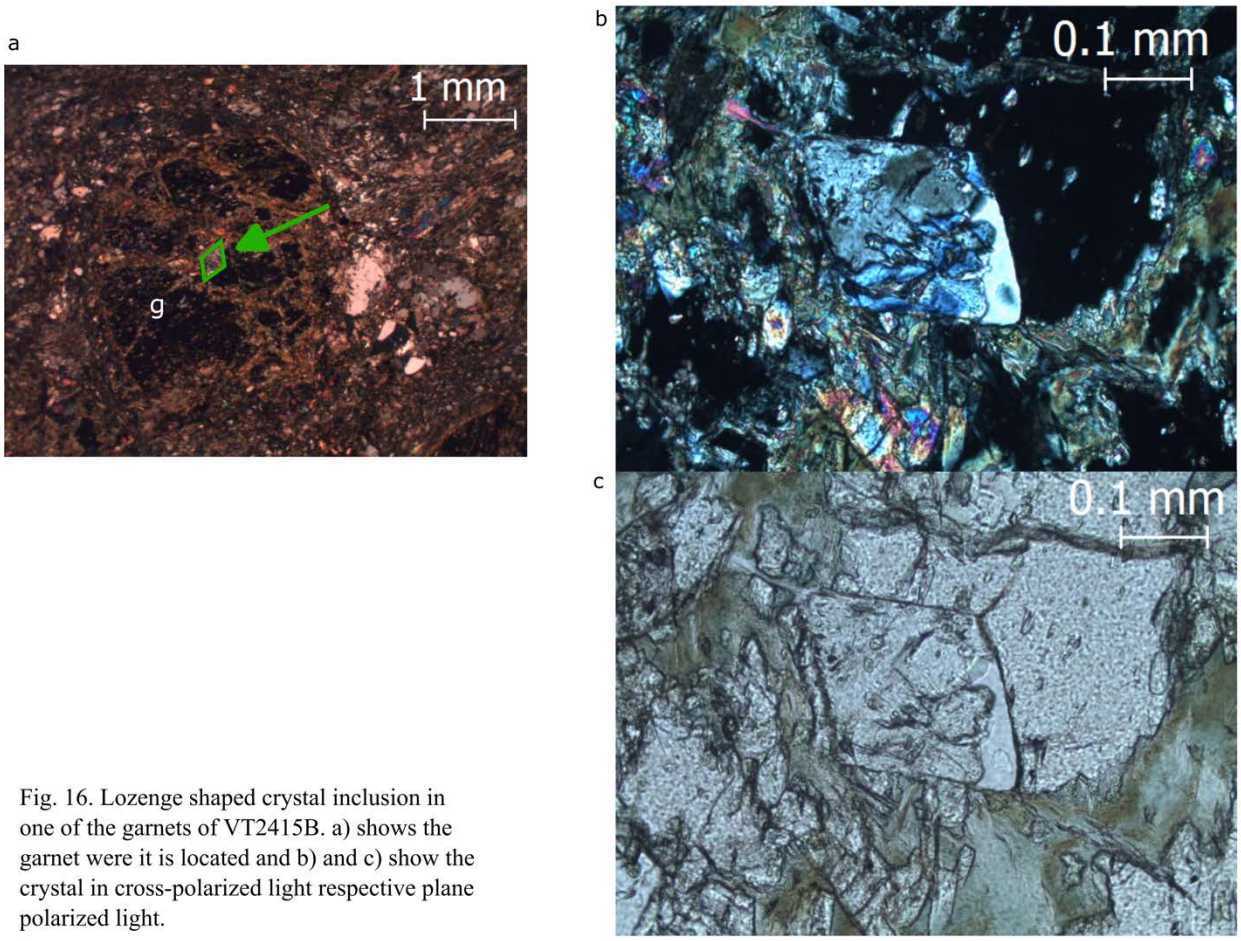

Fig. 16. Lozenge shaped crystal inclusion in one of the garnets of VT2415B. a) shows the garnet were it is located and b) and c) show the crystal in cross-polarized light respective plane polarized light.

5.2 Mineral chemistry

Two garnet porphyroblasts from sample VT2409B were quantitively analyzed by the electron microprobes WDS. These garnets are named VT2409B-1 and VT2409B-2 and the location of the grains in the sample is shown in Fig. 17.

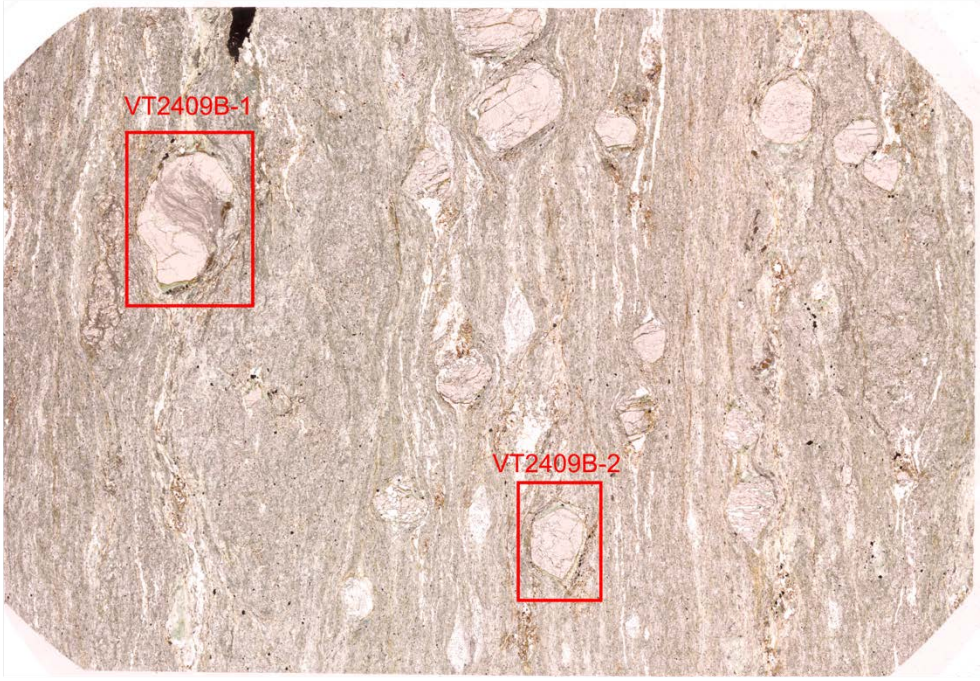

Fig. 17. Position of the garnets analyzed in sample VT2409B.

Two different strategies were used to analyze the two garnet porphyroblasts. Garnet VT2409B-1 contains numerous inclusions and cracks and therefore chemical analyses were acquired along three different sub-lines (Fig. 18a). The first and third sub-lines (79- and 37-point analyses, respectively) were run automatically using a step of 25 μm. The second line, which passes through an inclusions-rich garnet domain consists of manually placed spots. The VT2409B-2 profile, was run as one continuous profile (Fig. 18b) and consist of 86 punctual analyses programmed using a step of 25 μm.

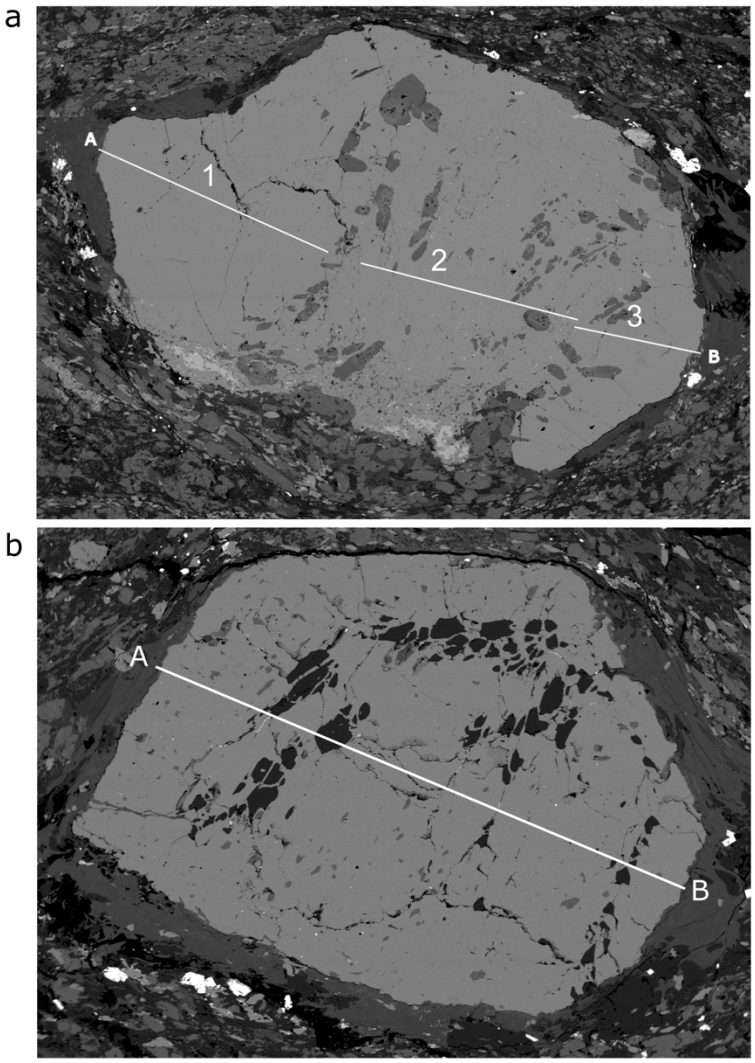

Fig. 18. a) Garnet VT2409B-1, showing the three segments of the profie analysed. b) Garnet VT2409B-2 continuous profile.

The chemical composition of garnet was recalculated and the end-members grossular, spessartine, almandine and pyrope are plotted in Fig. 19 (profile VT2409B-1) and Fig. 20 for (profile VT2409B-2). Certain points from these profiles were deleted as these corresponded with either being outside the garnet rim or going through other mineral inclusions. Such points were identified by either having (i) a silica content outside the garnet norm of 2.98–3.1 (atom per formula unit) a.p.f.u. or (ii) a together Ca and Ti concentration higher than what's expected of garnet. The higher Ca and Ti content indicate a mixed analysis with epidote and titanite inclusions.

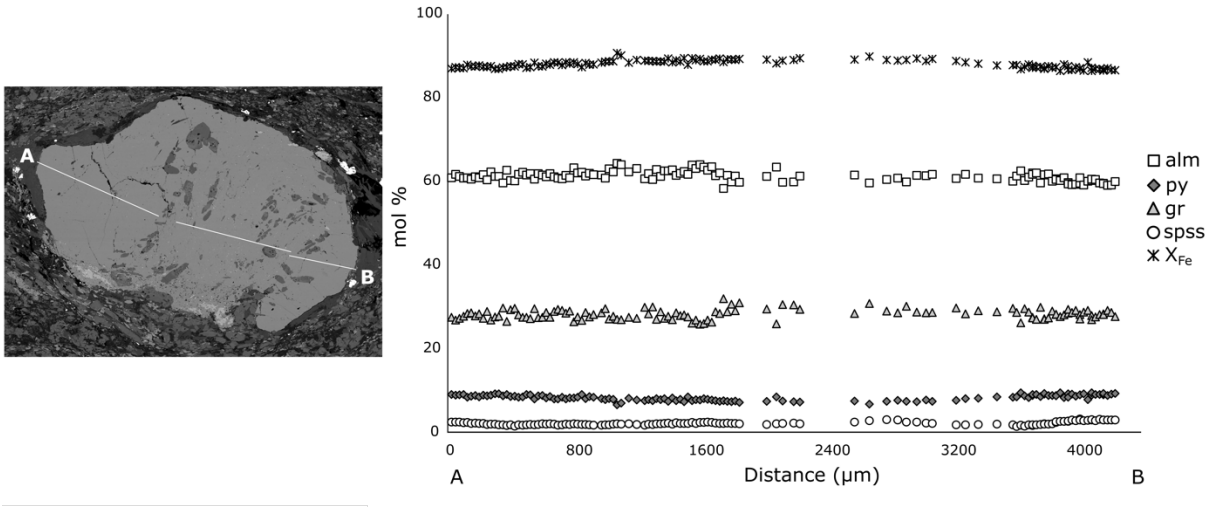

Fig. 19. Profile of garnet VT2409B-1, with its three segments seen in the EMPA image to the left, displaying the chemical composition throughout the grain.

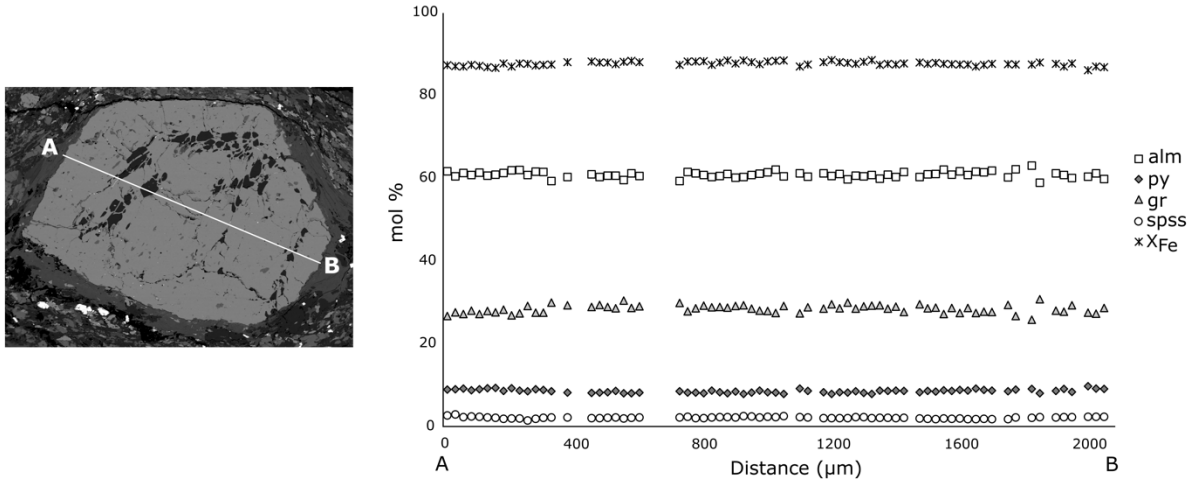

Fig. 20. Profile of garnet VT2409B-2 displaying the chemical composition throughout the grain.

Both garnet porphyroblasts display a similar and constant composition and thus are not chemically zoned. In detail, they display high almandine (60–63 mol.%) and grossular (27–30 mol.%) and low pyrope (8–9 mol.%) and spessartine (2–3 mol.%).

Further chemical analyses with WDS were applied on the selected minerals amphibole, white mica, chlorite, as well as the opaque Fe-oxides. The amphibole is Ca-rich with some Na in its composition. The white-mica, which has only been observed in the lozenge-shaped aggregates, consist of two different mineral phases, Si-rich muscovite and paragonite. The opaque minerals are magnetite and each of the mentioned minerals recalculated chemical composition expressed as wt.% can be found in Appendix 1 (Tab. A3).

No profile for the chemical composition of any of the garnets in sample VT2415B has been acquired from EPMA.

5.3 P–T conditions

A pseudosection was calculated using the bulk rock chemistry of sample VT2409B which is given in the Appendix 1 (Tab. A4). The total iron (expressed as Fe_2O_3) is equal to 10.61 wt%, whereas the measured amount of FeO is 6.49 wt%. Calculations were run in the *P–T* range 12–25 kbar and 400–600 °C (Fig. 21).

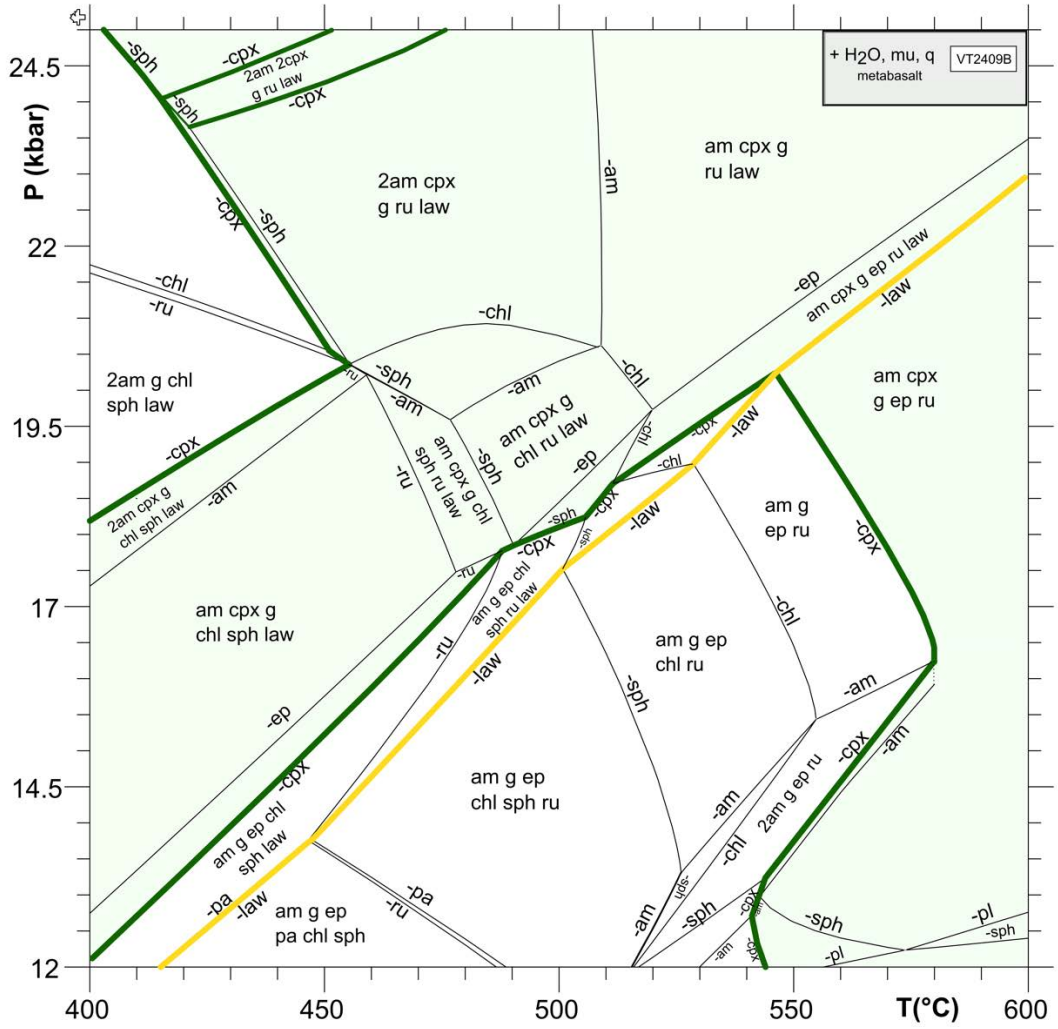

Fig. 21. Calculated pseudosection for sample VT2409B in the interval of 400–600 °C and 12–25 kbar. The fields where clinopyroxene is stable are depicted in light green, whereas the lawsonite-in line is depicted in yellow.

The lawsonite-in line is marked in yellow and divides the *P–T* space into two main domains, i.e. the one that contains lawsonite and the one that is lawsonite-free. In Fig. 21, the fields where clinopyroxene is stable are depicted in pale green. This mineral is not stable in two domains: the first one is comprised between 400–540 °C 12–19 kbar whereas the second one is comprised between 400–440 °C 18–25 kbar.

The observed mineral assemblage amphibole-garnet-epidote-titanite-rutile-lawsonite-quartz-muscovite is stable in a narrow field between 14–17 kbar and 460–500 °C (Fig. 22). The measured

modal abundance of garnet (~7 vol.%) well matches with the modelled one. Chlorite (4–6 vol.%, Tab. 2) is present in this field, but is not part of the observed peak assemblage. The model predicts the presence of an amphibole, the composition of which corresponds to a glaucophane, a sodic amphibole. In the investigated sample, only calcic amphibole was observed. The lack of glaucophane is attributed to the intense retrogression that affects the rock.

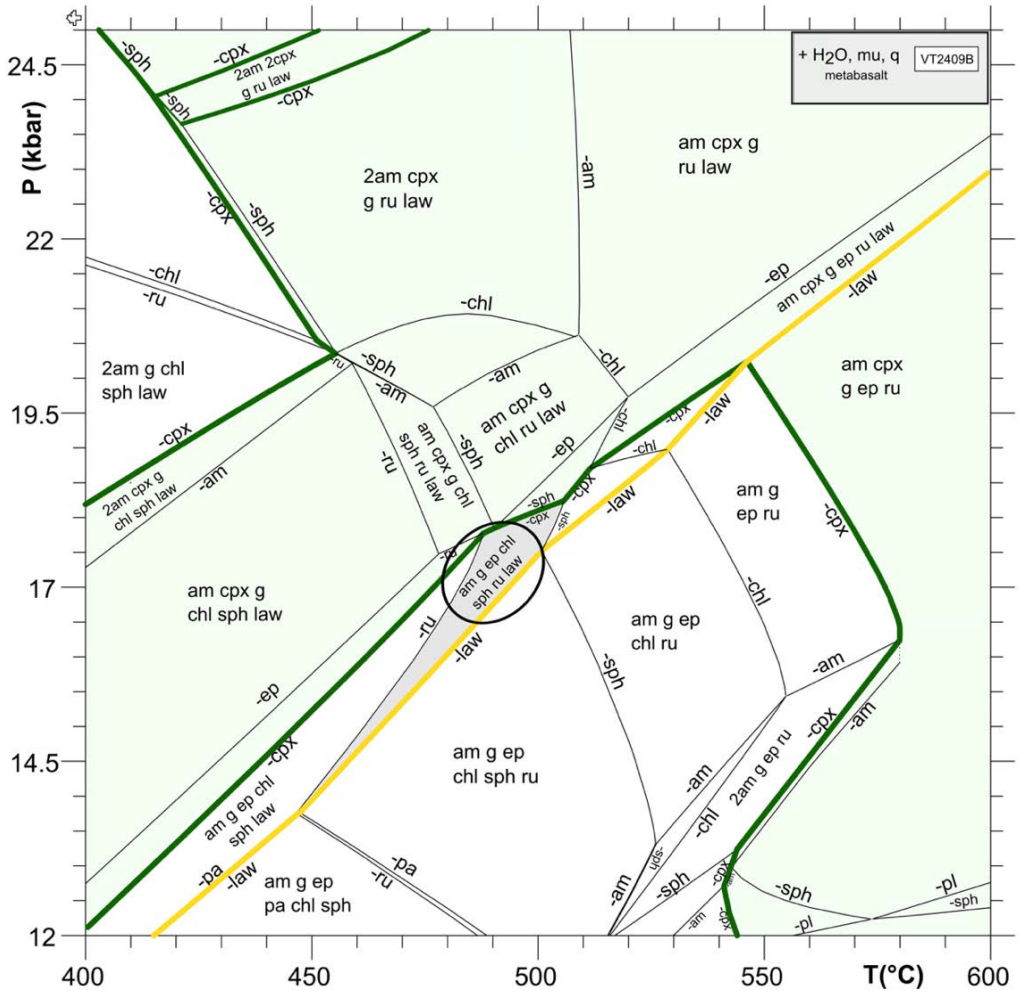

Fig. 22. The black ring marks the field in which the mineral assemblage am-g-ep-chl-sph-ru-law is stable and reassembles the observed mineral assemblage the closest.

P-T conditions		Mineral mode									
T (°C)	P (kbar)	am (gl)	g	ep	mu	chl	q	sph	ru	law	o
Low T domain											
490	**17**	46	2	21	6	6	7.5	2.4	0.7	7	
500	**17**	47	4.9	26	6.5	4.4	7.8	0.3	1.4	1.1	
High T domian											
570	**22**	31.7	16	3.2	6.7		8		1.6	19	14
580	**22.5**	28.6	17.7	2	6.7		8.4		1.6	18.9	15.9

Tab. 2 Modal abundances (in vol.%) of minerals calculated at different *P–T* conditions.

Fig. 23 reports the chemical isopleths for the garnet end-members (spessartine, pyrope and grossular).

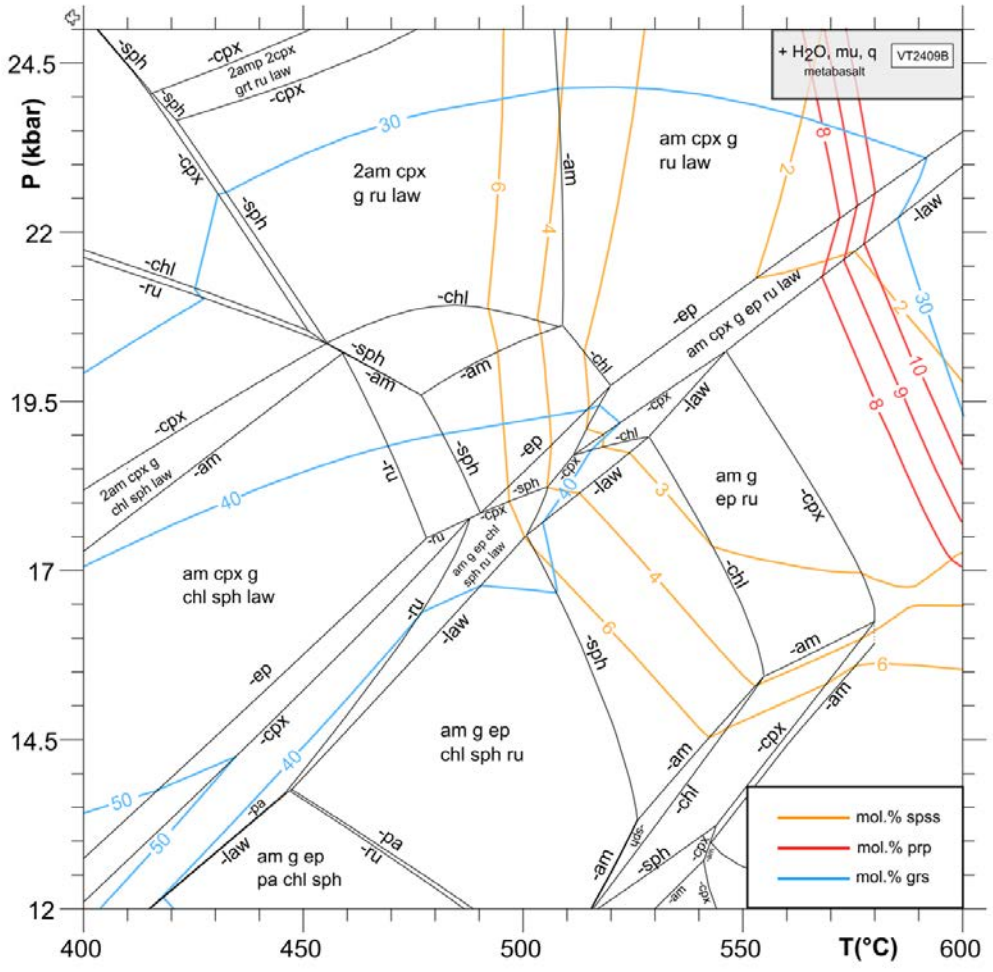

Fig. 23. The calculated endmember isopleths of garnet (spessartine, pyrope and grossular).

The measured garnet composition (grs = 27–30 mol.%, prp = 8–9 mol. %, spss = 2–3 mol.%) is predicted to be stable at 21–23 kbar and 560–580 °C, in the amphibole-clinopyroxene-garnet-epidote-rutile-quartz-muscovite field (Fig. 24). At these *P–T* conditions the model predicts the presence of clinopyroxene (14 to 16 vol.%, Tab. 2) and the absence of titanite and lawsonite. However, petrographic observations show that titanite and lawsonite were present during garnet growth (both as inclusions in garnet as well as in the matrix). By contrast, clinopyroxene is not observed in the studied sample.

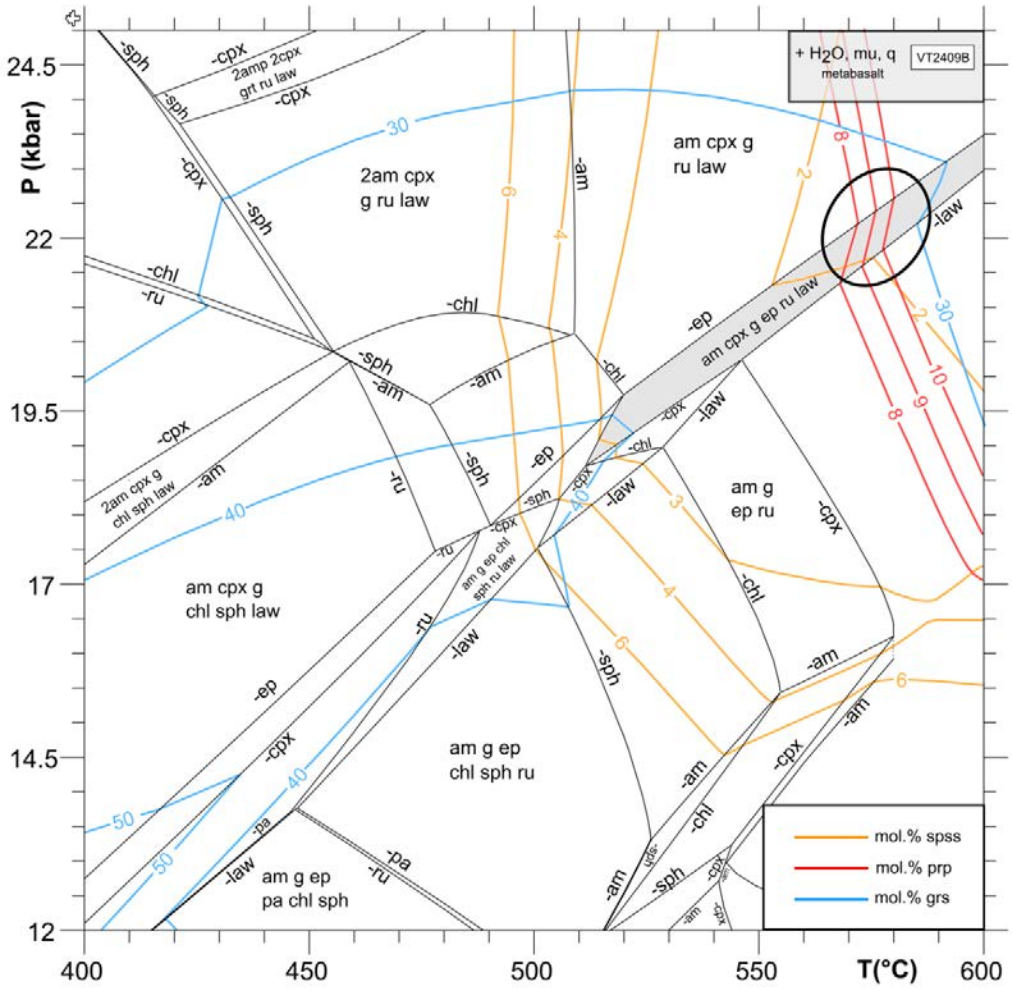

Fig. 24. The black ring marks the intersection of the garnet isopleth which matches the measured composition of the garnet obtained from EPMA. The grey area shows the mineral assemblage am-cpx-g-ep-ru-law in which the garnet isopleths intersect.

Paragonite and muscovite replaces lawsonite. Thermodynamic modelling indicates that paragonite is stable at 12–13 kbar and 420–450 °C in the amphibole-garnet-epidote-paragonite-chlorite-titanite-quartz-muscovite field (Fig. 25). At these *P–T* conditions, rutile and lawsonite are not any more stable. This is in line with petrographic observations which reveal (i) rutile crystals partially replaced by titanite and (ii) lawsonite pseudomorphed by paragonite and muscovite.

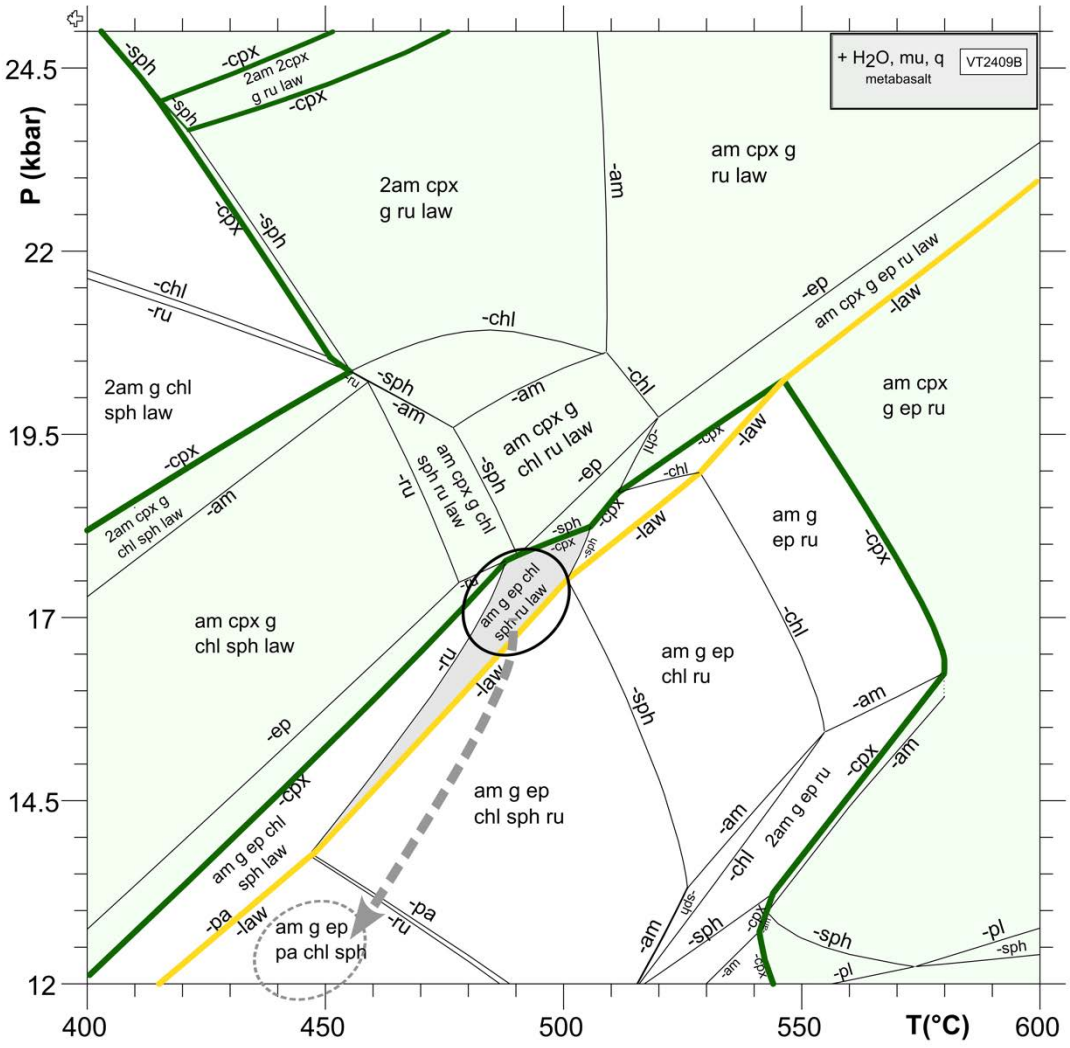

Fig. 25. The dashed line indicates the suggested path during exhumation into the am-g-ep-pa-chl-sph field (marked by the dashed grey circle).

6. Discussion and conclusions

This BSc thesis investigates a metabasalt (sample VT2409B) from the Piemonte-Liguria Ocean. This sample was collected in the Valtournanche valley in the Western Alps, where both blueschist and eclogite units belonging to the Piemonte-Liguria Ocean are well exposed. However, there is no general consensus if the sampling area belongs to the eclogite-facies Zermatt Zone or to the blueschist Combin Zone. In other words, the exact position of the tectonic boundary between these two units is disputed. Therefore, petrographic observations, mineral chemistry and thermodynamic modelling were applied in order to estimate the peak *P–T* conditions reached by the metabasalt VT2409B and to understand to which unit the sampling area belongs.

6.1 P–T evolution of the studied metabasalt

The early prograde Alpine history recorded by the studied metabasalt is associated with the mineral assemblage glaucophane-lawsonite-epidote-titanite-rutile-lawsonite-quartz-muscovite. Most of these minerals are preserved as inclusions in garnet, including perfect lozenge shape pseudomorphs after lawsonite. Glaucophane, a sodic amphibole, is not preserved, but it was pervasively replaced by a calcic amphibole during retrogression, a feature commonly observed in the rocks from the Combin Zone (e.g. Manzotti et al. 2021).

The peak mineral assemblage includes glaucophane-lawsonite-garnet-epidote-titanite-rutile-quartz-muscovite. Thermodynamic modelling (and more specifically the comparison between the modelled and observed mineral assemblage) constrains the peak *P–T* conditions at 14–17 kbar 460–500 °C. These *P–T* estimates suggests that (i) the studied sample belongs to the Combin Zone and thus (ii) the contact with the Zermatt Zone is located structurally below the collected sample (Fig. 26). These results agree with the interpretation of Dal Piaz et al. (2015) and Arienti et al. (2025): these authors attributed the sampling area to a slice of the Combin Zone, namely to the Combin Unit (Fig. 26).

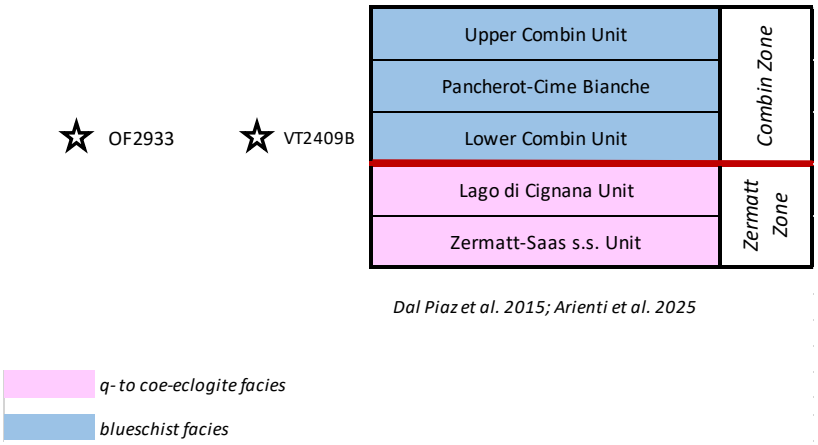

Fig. 26. Oceanic nappe stack in the Valtournanche valley according to Dal Piaz et al. (2015) and Arienti et al. (2025). Tectonic boundary (red line) between the Zermatt and Combin Zone. The white stars refer to the structural position where the metabasalt (sample OF2933) studied by Groppo et al. (2009) and the metabasalt (sample VT2409B) studied in this thesis was collected.

Finally, the studied metabasalt underwent intense retrogression during exhumation, as petrographically recorded by (i) pseudomorphs after lawsonite (containing paragonite and muscovite), (ii) the partial replacement of rutile by titanite and of garnet by chlorite and (iii) the complete replacement of sodic amphibole by calcic amphibole. Thermodynamic modelling indicates that these minerals formed during retrogression at 12–13 kbar 420–450 °C.

6.2 Comparison with previous studies

This BSc study is the first attempt to constrain the peak *P–T* conditions of this sampling area by thermodynamic modelling. However, previous petrological studies have been conducted on metasediments and metabasalts collected in the same structural position as the studied metabasalt VT2409B. Specifically, the maximum *T* (420–530 °C, Raman spectroscopy on carbonaceous material) estimated by Negro et al. (2013) on metasediments are consistent with the ones (460–500 °C) obtained in this study, using thermodynamic modelling.

The metabasalt (sample OF2933) investigated by Groppo et al. (2009) and the one studied in this BSc thesis display the same peak mineral assemblage. In addition, both show large garnet crystals, with similar chemistry (i.e. crystals show a very weak or even no chemical zoning) and they do not contain either fresh omphacite or omphacite pseudomorphs. Groppo et al. (2009) constrained the peak metamorphic conditions at ~24 kbar and ~600 °C, applying the empirical garnet-phengite thermometer and the Si content in phengite (Krogh & Råheim 1978 and Green & Hellman 1982). However, at these *P–T* conditions, omphacite should be present. The *T* estimated is 100 °C higher than the one estimated by Negro et al. (2013). It must be noted that the method used by Negro et al. (2013) is robust and provides the maximum *T* reached by a rock.

Interestingly, the intersection of the modelled chemical isopleths for garnet obtained in this BSc study occurs at *P–T* conditions (21–23 kbar, 560–580 °C) similar to the one of Groppo et al. (2009). The intersection of the chemical isopleths for garnet should provide the *P–T* conditions at which garnet grew. This approach is generally used to constrain the prograde segment of a *P–T* path, due to the fact that the chemical composition of garnet changes at increasing *P* and *T* conditions. However, this method is quite difficult to apply in the case of sample VT2409B as well as in the sample studied by Groppo et al. (2009), because garnet is not zoned (the chemistry does not change from core to rim). It is possible that this discrepancy between the modelled and measured garnet composition, can be lined to uncertainties of solid solution models, as reported in other studies (e.g. Manzotti et al., 2015; Giuntoli et al., 2018).

7. Future work

In this study, thermodynamic modelling (calculation of only one pseudosection) has been applied using the bulk rock composition and the *P–T* conditions have been established comparing the modelled and observed mineral assemblage. The discrepancy between the modelled and measured garnet composition need to be further explored. Thermodynamic modelling (i.e. calculation of isothermal P–*X* phase diagrams at the peak *T*) can be used to explore the role of certain elements (Fe^{3+}, Ca) on the stability of garnet. In addition, Raman spectroscopy on quartz inclusions in garnet (e.g. Ashley et al. 2014) can be used to estimate the entrapment *P* of these inclusions. This approach is based on the elastic properties of inclusions and their host and allows and estimation of P which is independent from the equilibrium thermodynamics approach used by Theriak/Domino, Thermocalc or Perplex.

8. Acknowledgments

I wish to express gratitude to my supervisor, Paola Manzotti, for her guidance and extensive feedback during the course of this thesis. I also extend my thanks to Daniel Buczko, operator of the electron microprobe at Uppsala Geocentrum, for carrying out the mineral analyses and providing valuable insights about EPMA.

9. References

Agard, P., 2021. Subduction of oceanic lithosphere in the Alps: selective archetypal from (slow-spreading) ocean. *Earth Sci Rev* 214:103517.

Alex Strekeisen. 2006-2020 microphotographs.
Lawsonite: https://www.alexstrekeisen.it/english/meta/lawsonite.php
Omphacite: https://www.alexstrekeisen.it/english/meta/omphacite.php
Garnet: https://www.alexstrekeisen.it/english/meta/garnet.php

Arienti, G., Bistacchi, A., Caumon, G., Monopoli, B., Dal Piaz, G., 2025. 3D structural implicit modelling of folded metamorphic units at Lago di Cignana with uncertainty assessment. *Journal of Structural Geology* **191**:105329.

Ashley, KT., Steele-MacInnis, M., Caddick, MJ. 2014 QuiB Calc: A MATLAB® script for geobarometry based on Raman spectroscopy and elastic modeling of quartz inclusions in garnet. *Computers & Geosciences* **66**:155–157

Ballévre, M., Merle, O., 1993. The Combin Fault: compressional reactivation of a late Cretaceous-Early Tertiary detachment fault in the Western Alps. *Sweizerische mineralogische und petrographische Mitteilungen*. **73**(2), 205-227.

Ballèvre, M., Pitra, P., Bohn, M., 2003. Lawsonite growth in epidote blueschists from the Ile de Groix (Armorican Massif, France): a potential geobarometer. *Journal of Metamorphic Geology*. **21**(7), 723-735.

Bousquet, R., Oberhänsli, R., Schmid, S.M., Berger, A., Wiederkehr, M., Robert, C., Möller, A., Rosenberg, C., Zeilinger, G., Molli, G., & Koller, F. (2012). Metamorphic framework of the Alps. *Commission for the geological map of the world; subcommission for magmatic and metamorphic maps. Paris: IUGS and IUGG*, Retrieved from: http://www.ccgm.org, 2012.

Bucher, K., Grapes, R. 2011. Petrogenesis of Metamorphic Rocks, 8th edition. Springer Berlin Heidelberg. (Earth and Environmental Science)

Cameca EPMA tutorial. 2018 John Wiley & Sons Ltd, The Atrium, Southern Gate, Chichester, West Sussex PO19 85Q, UK. Microscopy EKB Series Editor: Dr Julian Heath. Spectroscopy and separations EKB series editor: Arne Kusserow. Webadress: https://www.cameca.com/products/epma/epma-introduce

Carignan, J., Mevelle, G., Morel, J., Yeghicheyan, D. 2001. Routine analyses of trace elements in geological samples using flow injection and low pressure on-line liquid chromatography coupled to ICP-MS: a study of geochemical reference materials, BR, DRN, UB-N, AN-G and GH. *Geostandards and Geoanalytical Research*. **25**, 187-198.

Castelli, D., Rubatto, D., 2002. Stability of Al- and F-rich titanite in metacarbonate: petrologic and isotopic constraints from a polymetamorphic eclogite marble of the internal Sesia Zone (Western Alps). *Contributions to Mineralogy and Petrology*. **142**, 627-639.

Çetinkaplan, M., Candan, O., Oberhänsli, R., Bousquet, R. 2008. Pressure temperature evolution of lawsonite eclogite in Sivrihisar; Tavşanlı Zone Turkey. *Lithos*. **104**. 12-32.

Dal Piaz, G.V., Bistacchi, A., Gianotti, F., Monopoli, B., Passeri, L., Schiavo, A. 2015. Explanatory Notes of the sheet 070 Monte Cervino of the geological Map of Italy at 1:50,000 scale. Volume **101**, p. 272.

de Capitani, C. & Brown, T.H. 1987. The computation of chemical equilibrium in complex systems containing non-ideal solutions. *Geochimica et Cosmochimica Acta*. **51**, 2639-2652.

de Capitani, C. & Petrakakis, K. 2010. The computarion of equilibrium assemblage diagrams with Theriak/Domino software. *American Mineralogist*. **95**, 1006-1016.

Deer, W.A., Howie, R.A. & Zussman, J. 2013. An Introduction to the Rock-Forming Minerals. 3rd edition. Mineralogical Society.

Dey, A., Sen, K., Sen, A., Choudhary, S., 2023. Omphacite breakdown, symplectite formation and carbonate metasomatism in a retrograded continental eclogite: Implications for the exhumationof the Tso Morari Crystalline Complex (Trans-Himalaya, NW India). *Physics and Chemistry of the Earth, Parts A/B/C*. **131**:103453

Spear, F.S. (1993) Metamorphic Phase Equilibria and Pressure-Temperature-Time Paths. Monograph 1, Mineralogical Society of America, Chantilly, Virginia.

GeologyScience2018. https://geologyscience.com/rocks/metamorphic-rocks/foliated-metamorphic-rocks/blueschist/ Retrieved 2026-05-18.

Giuntoli, F., Lanari, P., Burn, M., Kunz, B. E., and Engi, M. 2018. Deeply subducted continental fragments – Part 2: Insight from petrochronology in the central Sesia Zone (western Italian Alps), *Solid Earth*, **9**, 191–222.

Green, T. H. and Hellman, P. L., 1982. Fe-Mg partitioning between coexisting garnet and phengite at high pressure, and comments on a garnet-phengite geothermometer. *Lithos*, **15**, 253–262.

Groppo, C., Beltrando, M., Compagnoni, R., 2009. The P-T path of the ultra-high pressure Lago di Cignana and adjoining high-pressure meta-ophiolitic units: insights into the evolution of the subducting Tethyan slab. *Journal of Metamorphic Geology*. **27**(3), 207-231.

Holland, T.J.B. & Powell, R. 2011. An improved and extended internally consistent thermodynamic dataset for phases of petrological interest, involving a new equation of state for solids. *Journal of Metamorphic Geology*. **29**, 333-383.

Konrad-Schmolke, M., Handy, M.R., Babist, J., O´Brien, J., 2005. Thermodynamic modelling of diffusion-controllod garnet growth. *Contributions to Mineralogy and Petrology.* **149**(2), 181-195.

Krogh, E. J. & Råheim, A., 1978. Temperature and pressure dependence of Fe-Mg partitioning between garnet and phengite, with particular reference to eclogites. *Contributions to Mineralogy and Petrology*. **66**, 75–80.

Manzotti, P., Ballèvre, M. 2024. Continental subduction in the Alps: from field data to kinematic models. Chapter 5, v.2. In: "Geodynamics of the Alps", Eds: Rosenberg, C., Bellahsen, N., Sciences – Dynamics of the continental lithosphere. Wiley, pp. 255-313.

Manzotti, P., Ballévre, M., Pitra, P., Schiavi, F. 2021. Missing lawsonite and aragonite found: P-T and fluid composition in meta-marls from the Combin Zone (Western Alps). *Contributions to Mineralogy and Petrology*. **176**(8):60.

Manzotti, P., Ballévre, M., Pitra, P., Putlitz, B., Robyr, M., Müntener, O. 2020. The Growth of Sodic Amphibole at the Greenschist- to Blueschist-facies Transition (Dent Blanche, Western Alps): Bulk-rock Chemical Control and Thermodynamic Modelling. *Journal of Petrology*. **61**. egaa044.

Manzotti, P., Ballèvre, M., Zucali, M., Robyr, M. & Engi, M. 2014a. The tectonometamorphic evolution of the Sesia–Dent Blanche nappes (internal Western Alps): review and synthesis. *Swiss Journal of Geosciences*. **107**, 309-336.

Manzotti, P., Pitra, P., Langlade, J., Ballèvre, M. 2015. Constraining P-T conditions during thrusting of a higher pressure unit over a lower pressure one (Gran Paradiso, Western Alps). *Journal of Metamorphic Geology*, **33**, 981–1002

Manzotti, P., Schiavi, F., *Nosenzo, F., Pitra, P., Ballèvre, M. 2022. A journey towards the forbidden zone: a new cold UHP unit in the Dora-Maira Massif (Western Alps). *Contributions to Mineralogy and Petrology*, **177**:59

Mindat.org https://www.mindat.org/photo-45288.html , copyright: Franz Bernhard. Retrieved 2026-05-18.

Negro, F., Bousquet, R., Vils, F., Pellet, C-M, Hänggi-Schaub, J. 2013. Thermal structure and metamorphic evolution of the Piemonte-Ligurian metasediments in the northern Western Alps. *Swiss Journal of Geosciences*. **106**, 62-78.

Lanari, P., Duesterhoeft, E. 2019. Modeling Metamorphic Rocks Using Equilibrium Thermodynamics and Internally Consistent Databases: Past Achievements, Problems and Perspectives. *Journal of Petrology*. **60**(1), 19–56

Philpotts, A.R. & Ague, J.J. (2022). Principles of Igneous and Metamorphic Petrology, 3rd edition. Cambridge: Cambridge University Press.

Reinecke, T. 1991. Very-high-pressure metamorphism and uplift of coesite-bearing metasediments from the Zermatt-Saas zone, Western Alps. European Journal of Mineralogy. 7-18.

Ring, U. 1995 Horizontal contraction or horizontal extension? Heterogeneous Late Eocene and Early Oligocene general shearing during blueschist and greenschist facies metamorphism at the Pennine-Austroalpine boundary zone of the Western Alps. *Geologische Rundschau*, **84**:843–859

Schulte, B., Sindern, S. 2002. K-rich fluid metasomatism at high-pressure metamorphic conditions: Lawsonite decomposition in rodingitized ultramafite of the Maksyutovo Complex, Southern Urals (Russia). Journal of Metamorphic Geology. **20**(6):529-541.

Tajčmanová, L., Manzotti, P., Alvaro, M. 2021 Under pressure: high-pressure metamorphism in the Alps. *Elements* **17**:17–22

Winter, J.D. 2010. Principles of Igneous and Metamorphic Petrology, 2nd edition. Prentice Hall.